NTNU

Norwegian University of
Science and Technology

Cooling of Transducer array used for Ultrasound radiation Force

Håkon Risbakk

Cooling of transducer array used for Ultrasound Radiation Force

Håkon Risbakk

Department of Physics

NTNU, Norwegian University of Science and Technology

August 14, 2015

Preface

This thesis is submitted to the Norwegian University of Science and Technology (NTNU) for the degree of Master of Science during 2015.

The work has been carried performed at the Department of Physics, NTNU, Trondheim, with supervison from Catharina de Lange Davies, Professor in the Department of Physics at NTNU, and co supervisors Bjørn Angelsen Department of Circulation and Medical Imaging, at NTNU, and Tonni Franke Johansen SINTEF.

Summary

This thesis reviewed the power requirements for high Ultrasound Radiation Force apparatus, and the heat generation caused by this.

This thesis proposed a way to cool an ultrasound transducer. The cooling method is to have a an area on the casing of the transducer that has a high thermal conductivity, and a high emissivity. This layer is meant to passively transfer heat from the casing to the surroundings. This area on the casing is connected to the transducer stack through a copper layer that is separated for the stack by thermal paste. This cooling method was simulated using a two step method. The first step was to determine the amount of heat transferred from the highly conductive area on the casing to the surrounding, assuming constant surface temperature. The second step was to simulate the heat transfer from the transducer stack to the casing assuming evenly distributed constant heat generation in the transducer stack.

The conductive casing that was simulated was a prism surrounding the sides of the transducer stack, but not the top and bottom. This prism was off height 4cm. It was found that the casing material should have as high conductivity and emissivity as possible in order to increase heat transfer. The thickness of thermal paste was found to have a large impact on the heat transfer from the transducer stack to the conductive casing. Thisnecessitates care when applying thermal paste to make sure it has the desired thickness.

The warmest area of the transducer would based on the simulations be close to the backing. In order to increase heat transfer out of the transducer, it was therefore proposed to add a thermal conductive layer just above the backing off the transducer. This method was shown in simulations to be effective in increasing heat transfer. With this added thermal conductive layer the transducer would stabilize around $56C^o$ for a heat generation of 8.3W evenly distributed throughout the transducer.

Sammendrag

Denne masteroppgaven gjennomgått kravene til høy effekt for transducere som produser høy strålingskraft. Den har også gått igjennom hvordan dette påvirker varmegenerering.

Denne masteroppgaven har foreslått en måte å kjøle en ultralydtransducer. Kjølmetoden er å ha ett område på skallet rundt transduceren som har køy varmelednings evne og høy emmisivitet. Dette laget er koblet til transducere gjennom ett kobberlag og ett lag med kjølepasta. Denne kjølemetoden ble simulert med en to trinns metode. Det første steget var å simuelere varmeoverføring mellom skallet og omgivelsene, med anntagelsen om konstant skalltemperatur. Steg to var å simulere varmeoverføringen fra ultralydtransduceren til skallet, med antagelsen om konstant varmegenerering gjevnt fordelt i transduseren.

Den høyt varmeledende delen av skallet var formet som ett prisme som omga transduceren på alle kanter bortsett fra over og under. Dette prismet var 4 cm høyt. Det ble funnet at dette varmeledende materialet burde ha så høy varmeledning og emmisivitet som mulig for å øke varmeledning. Tykkelsen på kjølepastaen viste seg å ha stor innvirkning på varmeoverføringen mellom transduseren og skallet.

Det varmeste området i transduceren ble i simmuleringene funnet å være nært backingen. For å øke varmeoverføringen til skallet ble det derfor forsøkt å legge til ett ekstra varmeledningslag mellom backingen og resten av transduceren. Dette viste seg å ha god innvirkning på varmeoverføringen til skallet. Med dette ekstra varmeoverføringslaget stabiliserte transduseren seg rundt $56C^o$ ved en varmegenerering på 8.3W.

Acknowledgement

I would like to thank the following people for their help during this project:

First, my supervisors, Professor Bjørn Angelsen Department of Circulation and Medical Imaging, at NTNU. Professor Catharina de Lange Davies, Department of Physics at NTNU, Department of Circulation and Medical Imaging. Tonni Franke Johansen at SINTEF. This thesis would not be possible without their help.

I would like to than my partner Nathalie Marquesin de Oliveira, for her invaluable assistance and support. I would like to thank my friends Håkon Seljåsen and Leif Kristian Tungodden , for their help during my studies.

CONTENTS

1. INTRODUCTION

This master thesis is a part of a project to create ultrasound mediated drug delivery at the Norwegian University of Science and Technology (NTNU). This project intends to use microbubbles consisting of a shell containing drugs, to deliver chemotherapy. [20] states that the typical microbubbles for ultrasound contrast have a diameter round 2μm. [21] discusses contrast microbubbles in the 1-2μm, 4-5μm and 6-8μm ranges. Ultrasound will then be used to direct these microbubbles to their destination, burst them as well as continually image the body. This sets stringent requirements on the ultrasound transducer.

This thesis focuses on evaluating the heat transfer in the ultrasound transducer. There are components in the transducer that can take damage from as low as 60 degrees. Making sure that the heat produced in the transducer is removed is important.

Aggressively growing cancer tumors often have a chaotic organization of capillaries with imperfect, highly permeable capillary walls. This wall imperfection allows the passage of nano-particles containing chemotherapy, while not crossing normal tissue Hence protecting normal tissue against the drug. However, the increased wall permeability also gives a high leakage of fluid from the blood into the interstitium (space between cells), which combined with a weak lymphatic drainage produces an increased interstitial pressure with low pressure gradient convection of nano-particles and also free drug molecules from the capillaries and deep into the interstitum.

Ultrasound radiation force (URF) provides a similar force on fluids and particles as a pressure gradient, and can be used to increase the transport of drugs and particles from the capillaries and deep into the interstitium. The radiation force is proportional to the extinction of the acoustic radiation intensity through scattering and thermal absorption due to particles and large molecules in the fluid. To obtain a large radiation force it is necessary to transmit a high acoustic intensity, which presents challenges to reduce absorption in the transducers. It is also necessary to provide heat conduction from thermal sources and cooling of the transducer. The scattering and absorption is

also frequency dependent, so that an optimal frequency for maximal radiation force depends both on particle type and depth of the tumor.

The work contains the following parts:

1. Review of the high power requirements for URF, and the heat generation caused by this.

2. Establish model for heat generation and thermal conduction of the complete array, where structures for cooling of the array is included. Develop a computer simulation model for this structure and simulate temperature developments in the array when heat is generated.

3. Design cooling structures from the simulations for increased power operation of the arrays.

2. THEORY

2.1 Cancer

About 8.5 million deaths were caused by cancer in 2012 [28]. This accounts for 14.6% of all human deaths in that year.

Six hallmarks of cancer has been proposed by [22], sustaining proliferative signaling, evading growth suppressors, resisting cell death, enabling replicative immortality, inducing angiogenesis and activating invasion and metastasis.

1. Sustaining proliferative signaling: In healthy tissue there is a well regulated process of activating proliferative signals when needed and deactivating them when not needed. The result is that healthy tissue has a homeostasis of cell numbers, and that normal tissue architecture and function is maintained. In cancer cells this regulation does not work, and there are much higher levels of proliferate signals.

2. Evading growth suppressors: There are many mechanisms to suppress cell growth that gets activated as a result of the sustained proliferative signaling. In order for the tumor to grow these mechanisms have to be evaded.

3. Resisting cell death, resisting apoptosis. Cells in tissue are highly organized, and their numbers are tightly regulated. This regulation happens both due to control off the amount of new cells created, and by planned cell death or apoptosis. This cell suicide can is quite common, in healthy humans billions of cells die every hour in the bone marrow ad the intestine [16]. Apoptosis is an important natural barrier to cancer development. In order for a tumor to become high grade malignant apoptosis has to be avoided.

4. Enabling replicative immortality: Most healthy cells are only able to pass through a limited number of successive cell growth-and-division cycles. However cancer cells require unlimited replicative potential in order to create macroscopic tumors. The

end of chromosomes are protected by telomeres, to hinder degradation and illegitimate recombination [15]. states that For every cell growth-and-division cycle these telomeres are shorten until they become so short that copying the chromosome can not happen without mistakes. In most cancer cells however there are functionally significant levels of telomerase, a DNA polymerase that add telomere repeat segments to the ends of telomeric DNA [22]. The erosion of telomeres as a result of the growth-division cycle are therefore countered in these cells, leading to replicative immortality.

5. Inducing angiogenesis: The formation of new blood vessels (Angiogenesis), is a necessity in cancer tissue. As other cells, cancer cells require a supply of oxygen and nutrients, and evacuation of metabolic wastes and carbon dioxide. In the absence of angiogenesis tumors are, due to their proliferative capabilities, supply restricted, and therefore their growth is also limited. Cancer tissue overcome this obstacle by reducing the production of angiogenic inhibitors (anti-angiogenic), and increasing production of inducers (pro-angiogenic). An important part of this process is the increased production of Vascular Endothelial Growth Factor (VEGF).

6. Activating invasion and metastasis. Tumors are able to invade surrounding tissue, and to spread to far away tissues.

2.2   Chemotherapy

"This section discusses how chemotherapy works and the negative consequences of the treatment. This section also discusses how the low pressure gradient in cancer cells affect drug delivery.

Chemotherapy is a commonly used treatment for cancer. Chemotherapeutic agents are normally cytotoxic. This means that they target and kill cells that divide rapidly. Cancer cells fit this description, but they are not the only ones. Cells in the bone marrow, digestive tract and hair follicles also divide quickly and are therefore targeted. Myelosuppression is the decreased production of cells in the bone marrow. These cells include leukocytes, erythrocytes and thrombocytes. Leukocytes are responsible for providing immunity, erythrocytes are responsible for oxygen transportation in the blood and thrombocytes are responsible for normal blood clotting. The targeting of these cells by chemotherapeutic agents therefore have severe effects on the bodies

ability to handle infections, stop bleedings and supplying the cells in order to keep a normal cell activity level. As a result patients often have to be hospitalized under strict infection control, and treated with aggressive doses of antibiotics if there are signs of infection. Anemia resulting from the reduced production of erythrocytes, can greatly reduce the energy levels of the patients. Reducing the adverse effects of cancer treatment is of great importance.

In normal tissue the vasculature is orderly and efficient. There is a clear separation of arteries, arterioles and capillaries. These are evenly spread out. This is not true for cancer tissue, due to the high levels of VEGF . The vasculature in cancer tissue is disorganized. There is no clear distinction between arterioles capillaries and venules. Blood vessels in cancer tissue is also more permeable than in normal tissue. Lymphatic vessels show similar changes. Blood vessels have changing diameters, uneven shapes and can have dead ends. [27] The result of this is that the interstitial pressure in cancer tissue is higher than normal and that there is an increased geometric resistance.

The increased interstitial pressure caused by angiogenesis, leads to problems with delivery of chemotherapeutic agents to cancer tissue. The reason for this is that the differential pressure is smalll compared to normal tissue [19]. This causes osmosis to be the major delivery agent of the drug. In order to increase the differential pressure professor Bjørn Angelsen at NTNU has proposed to use high radiation force ultrasound.

2.3   General Ultrasound theory

This section will briefly discuss acoustic wave propagation in tissue. The main source of this information is [11] To get more in depth knowledge of this topic the reader is encouraged to read this book.

Ultrasound waves are pressure waves. These waves are primarily longitudinal in biological tissue, as transverse waves are heavily attenuated. In ultrasound waves differences in pressure cause movement of particles, which again causes differences in pressure. This is analogous to a spring mass system. The deviation of pressure from the average is analogous to the deviation of the mass from the resting position. The average speed of particles in an area is analogous to the speed of the mass in the

spring mass system. [30]

A particle has the equilibrium position $\vec{r}$. During vibration of the tissue this particle is moved to the position $\vec{r}_L$

$$\vec{r}_L = \vec{r} + \overrightarrow{\psi(\vec{r},t)} \tag{2.1}$$

Here $\overrightarrow{\psi(\vec{r},t)}$ is the displacement of the particle from its equilibrium position. The vibration velocity and acceleration of this particle is

$$\overrightarrow{u(\vec{r},t)} = \frac{\partial \overrightarrow{\psi(\vec{r},t)}}{\partial t} \tag{2.2}$$

$$\overrightarrow{a(\vec{r},t)} = \frac{\partial \overrightarrow{u(\vec{r},t)}}{\partial t} \tag{2.3}$$

This is the Lagrange description of vibrations.

In a homogeneous isotropic material the wave equation for pressure p and vibration speed $\vec{u}$ are respectively:

$$\nabla^2 p(\vec{r},t) - \frac{1}{c^2}\frac{\partial^2 p(\vec{r},t)}{\partial t^2} = 0 \tag{2.4}$$

$$\nabla^2 \overrightarrow{u(\vec{r},t)} = -\frac{1}{c^2}\frac{\partial^2 \overrightarrow{u(\vec{r},t)}}{\partial t^2} = 0 \tag{2.5}$$

here $c = \frac{1}{\sqrt{\rho\kappa}}$ is the speed of sound. ρ is the density of the medium and κ is the bulk compressibility.

2.4 Ultrasound radiation force

Acoustic waves produce a radiation force. [10] gives the ultrasound radiation force on a smalll volume ΔV as

$$\Delta F = \frac{\sigma_e I}{c}\Delta V \tag{2.6}$$

, where σ_e is the extinction cross section, c is the ultrasound propagation velocity, and I is the ultrasound intensity. $\sigma_e = \sigma_a + \sigma_s$, σ_a is the absorption cross section, σ_s

is the scattering cross section. The average ultrasound intensity is given as.

$$I = \frac{P2}{2Z_o} \tag{2.7}$$

where P is the pressure amplitude, and Z_o is the characteristic impedance of the medium. In the vicinity around the tumor it is desired to have $\frac{\Delta F}{\Delta V}$ as large as possible in order to increase the flow through the tumor. σ_e is frequency dependent and one can optimize the frequency in order to increase $\frac{\Delta F}{\Delta V}$. For this thesis the most relevant part is that $\frac{\Delta F}{\Delta V} \propto P^2$.

V_t is the voltage amplitude applied to the transducer, ω_o is its frequency, W_{it} is the effect applied to the transducer, W_{ot}.

[10] gives:

$$P_t = Z_0 H_{tt}(\omega_0) V_t \tag{2.8}$$

$$W_{it} = N_{el} \frac{|V_{it}|^2}{2|Z_{el}(\omega_o)|} cos(\Theta_{el}(\omega_o)) \tag{2.9}$$

$$W_{ot} = N_{el} A_{el} \frac{|P_t(\omega_0)|^2}{2Z_0} = N_{el} A_{el} \frac{Z_0^2 |H_{tt}(\omega_0)|^2 |V_t|^2}{2Z_0} = N_{el} A_{el} \frac{Z_0}{2}(\omega_o)|H_{tt}|^2 |V_t| \tag{2.10}$$

, here N_{el} is the number of elements in the transducer, Z_{el} is the electric input impedance of the element whit phase Θ_{el}. A_{el} is the radiation area of the transducer element. H_{tt} is the transfer function from element voltage to surface vibration velocity.

The power left as heat in the transducer when running is

$$W_{qr} = W_{it} - W_{ot} = \left(\frac{cos(\Theta_{el}(\omega_o))}{|Z_{el}(\omega_o)|} - A_{el} Z_0 |H_{tt}(\omega_0)|^2 \right) \frac{1}{2} N_{el} |V_t|^2 \tag{2.11}$$

$$= \left(\frac{cos(\Theta_{el}(\omega_o))}{|Z_{el}(\omega_o)| Z_0^2 |H_{tt}|^2} - \frac{A_{el}}{Z_0} \right) \frac{1}{2} N_{el} |P_t(\omega_0)|^2 \tag{2.12}$$

A transducer will not run continuously, it will run in pulses. T_p is the length of a pulse and T_r is the time between the start of one pulse to the start off the next pulse.

The average heat power to the assembly will then be:

$$W_{qAvg} = W_{qr}\frac{T_p}{T_r} \tag{2.13}$$

When using URF for drug delivery it is desired to have $\frac{\Delta F}{\Delta V}$ as large as possible. From equations 2.6, 2.7, 2.12 and 2.13 it is shown that

$$\frac{\Delta F}{\Delta V} \propto W_{qAvg} \tag{2.14}$$

Therefore, heating of the transducer will create a constraint on the amount of URF that can be used for treatment.

2.5   Heat and Temperature

Temperature is a measure of the average internal kinetic energy of particles or molecules in a substance. This is related to the human sense of hot and cold. The main source for this section is [17]

Heat is the transfer of internal kinetic energy, or thermal energy. How much heat is required to change the temperature of a substance by a certain amount is material specific. The relationship is

$$\frac{Q}{mc} = \Delta T \tag{2.15}$$

where Q is the heat, m is the mass of the substance that receives the heat, ΔT is the change in temperature and c is a material dependent and empirical value, which for smalll changes in T can be considered constant. The value c is called the specific heat of a substance and has the unit $\frac{J}{kg \cdot K}$

Heat can also be expended or derived from a phase change in a substance, such as a solid liquefying, a liquid evaporating or the reverse processes. In this case the relationship is

$$Q = \pm mL \tag{2.16}$$

m is again the mass of the substance changing state, L, $[\frac{J}{kg}]$is an empirical value for the phase change, the sign depends on the direction of the phase change. In a transducer phase changes would cause grave problems and likely ruin the device. It is therefore important to avoid overheating.

2.6   Heat Transfer

Heat transfer refers to the transfer of thermal energy. There are three modes of heat transfer:

a) Conduction, relating to the transfer of heat due to random molecular motion.

b) Convection, relating to the transfer of heats due to a combination of diffusion and bulk movement of substances, this is common in liquids and gases.

c) Radiation, relating too the transfer of heat as photons.

2.6.1   Conduction

Conduction is due to random molecular movement. In solids this means lattice vibrations and movement of electrons. In a cube with surfaces of 1 m^2. (PICTURE) Two surfaces of this cube opposite to each other are held at constant temperatures T_1 and T_2, where $T_1 > T_2$. The other surfaces are completely insulated so that no heat can pass through them. The cube is made of a solid material. In this situation we will have a one dimensional heat transfer between surface 1 and 2. Since the cube is made of a solid material this heat transfer will be through conduction. The rate of heat transfer will be

$$q = \frac{dQ}{dt} = -kA\frac{T_2 - T_1}{L} = -kA\frac{\Delta T}{L} \tag{2.17}$$

where A is the surface area, L is the length between the surfaces, and k is the heat conductivity of the material. k has the unit $\frac{W}{m \cdot K}$ and is approximately constant for smalll changes in temperature.
For 3D situations the heat transfer is defined as the following relation [17]:

$$\vec{q}'' = \frac{d\vec{Q}}{dtdA} = -k\nabla T \tag{2.18}$$

2.6.2   Convection

Convection is term for heat transfer taking place when there is both diffusion of heat and bulk movement of substances. This is the situation for heat transfer in gases and liquids. Even if there is no forced movement the density changes that result from temperature changes will cause movement in the gas or liquid. For a surface, at

temperature T_s in contact with a fluid or gas whose temperature far away from the surface is T_∞, the following relation for the heat transfer. [17]

$$q^{''} = h(T_s - T_\infty) \tag{2.19}$$

This relation is known as Newton's law of cooling. h $[\frac{W}{m \cdot K}]$ is the convection heat transfer coefficient, which depends on the fluid properties, the surface geometry and the fluid motion.

Free convection

For the specialized case of a vertical plate with no forced convection, the convection heat transfer coefficient is given as

$$\bar{h} = \frac{\bar{Nu}_L \cdot k}{L} \tag{2.20}$$

, where k is the heat conductivity of the fluid surrounding the surface, L is the height of the plate and $\bar{Nu}_L$ is the Nusselt number given as [14]

$$\bar{Nu}_L = 0.68 + \frac{0.670 Ra_L^{\frac{1}{4}}}{[1 + (0.4925/Pr)^{9/16}]^{4/9}} \tag{2.21}$$

This equation is accurate for laminar flow, which is true for $Ra_L < 10^9$. Otherwise the following equation is used.

$$\bar{Nu}_L = \left\{ 0.825 + \frac{0.387 Ra_L^{\frac{1}{6}}}{[1 + (0.4925/Pr)^{9/16}]^{8/27}} \right\}^2 \tag{2.22}$$

Ra_L is the Rayleigh number a dimensionless number measuring the buoyancy driven flow.

$$Ra_L = \frac{g\beta(T_S - T_\infty)L^3}{\nu\alpha} \tag{2.23}$$

$\nu \ [m^2/s]$ is the kinematic viscosity. $\alpha \ [m^2/s]$ i the thermal diffusivity.
$\beta \ [k^{-1}]$ is the volumetric thermal expansion coefficient defined as

$$\beta = -\frac{1}{\rho}\left(\frac{\partial\rho}{\partial T}\right)_P \tag{2.24}$$

for ideal gases this is simply:

$$\beta = \frac{1}{T} \tag{2.25}$$

Pr is the prandtl number, the ratio between momentum and thermal diffusivity.

$$\beta = \frac{\nu}{\alpha} \tag{2.26}$$

2.6.3 Radiation

All mater at nonzero temperatures emits photons. The energy emitted by a surface is described by the surfaces emissive power $E[\frac{W}{m^2}]$, this is given by the Stefan-Boltzmann law as

$$E = \epsilon\sigma T_s^4 \tag{2.27}$$

$\sigma = 5.67 \cdot 10^{-8} \frac{W}{m^2 \cdot K^4}$ is the Stefan-Boltzmann constant. T_s is the surface temperature in Kelvin. ϵ is a material specific constant between 0 and 1 called *emissivity*. As well as emitting radiation, a surface will absorb radiation from its surrounding. All of the incoming radiation will not be absorbed, but only a fraction denoted by α. A gray surface is an idealized surface whose emissivity does not depend on the angle of radiation and independent of wavelength [24]. For a grey surface, $\epsilon = \alpha$ [17]. At temperature T_s with a surrounding at T_{sur} the net rate of radiation heat transfer $q^{''}$ is given as

$$q^{''} = \epsilon\sigma(T_s^4 - T_{sur}^4) \tag{2.28}$$

If there is a light source shining on the surface with irradiance I, the following equation applies:

$$q^{''} = \epsilon\sigma((T_s^4 - T_{sur}^4) - I) \tag{2.29}$$

A demonstration of the importance of the emissivity is given by the Leslie cube. The cube is filled with hot water. All the surfaces have the same temperature. However the different surfaces of the cube have different emissivities and therefore the radiation from these surfaces are different. In 2.1 one side is painted black, one is painted white and the other sides are of polished aluminum. The figur 2.1 shows the surface material has a large impact on the thermal radiation.
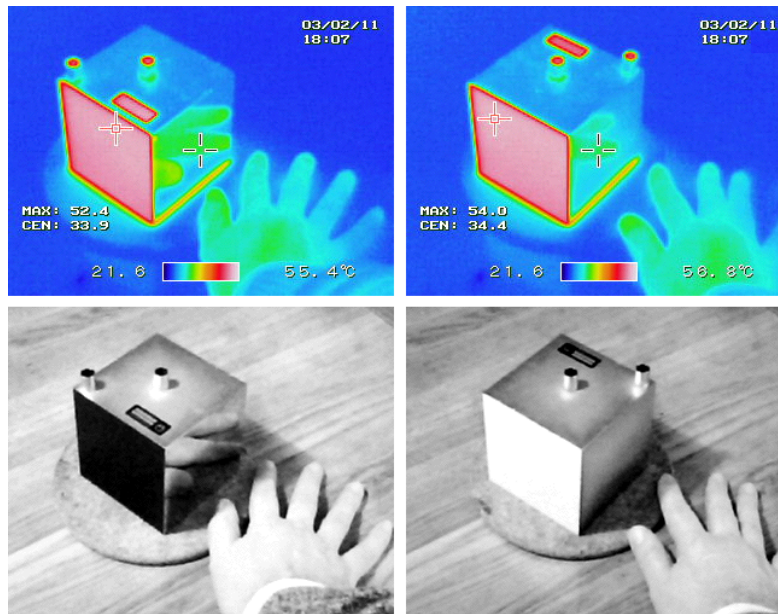
Fig. 2.1: Leslie Cube, picture wikimedia commons.

2.7 The Finite Element Method (FEM)

"The finite element method (FEM) has become one of the most frequently used methods for solving equations from mechanics of solids and fluids and thermodynamics that describe the behavior of physical systems in the form of partial differential equations" [18]. An essential characteristic of FEM is mesh discretization of a continous domain into smalller discrete sub-domains called elements [12]. The answers given by FEM simulations will get more accurate the finer the element mesh is made [13].

2.7.1 The Heat Equation

The heat equation or the heat diffusion equation is the equation that forms the basis for FEM i heat transfer. It is a combination of the conduction formula 2.18 and conservation of energy applied to a small control volume.

A medium is divided into a set of smalll cubes. The heat transfer in each of these cubes will be described by the conservation of energy in these cubes, and by equation

2.18. Conservation of energy says for one cube is given by the following expression:

$$\dot{E}_{in} + \dot{E}_g - \dot{E}_{out} = \dot{E} \tag{2.30}$$

In words: the change of energy in an element $\dot{E}$ is equal to energy that flows in to the element $\dot{E}_{in}$ + the energy that is generated in the element $\dot{E}_g$ minus the energy that flows out of the element $\dot{E}_{out}$. The internal energy of the element due to its temperature is proportional to the mass of the element $dm = \rho dV$, and to the specific heat of the substance c_p

$$\dot{E} = \rho c_p \frac{\delta T}{\delta t} dV = \rho c_p \frac{\delta T}{\delta t} dx dy dz \tag{2.31}$$

The energy that is created in the element can come from a variety of sources, electrical, chemical, acoustical. These will all be summed and described as $\dot{q}$. The generated energy is then given as

$$\dot{E}_g = \dot{q} dV = \dot{q} dx dy dz \tag{2.32}$$

Fourier's partial differential equation

$$\rho c_p \frac{\delta T}{\delta t} = div(k\nabla T) \tag{2.33}$$

must be satisfied at every point and at every time. And forms the basis of the FEM method for heat transfer for a time varying solution. [26]

2.8   Cooling methods

Cooling methods can be divided into two categories: passive cooling and active cooling. Active cooling methods refer to methods where one uses energy in order to lead to heat transfer. Passive cooling refers to methods where energy is not used to increase heat transfer. During the process of leading heat out of the system there is first an internal phase where the energy is transfered to the boundaries of the system and then an external phase where the energy is transfered from the boundary of the system to the environment. The first stage is achieved through coduction, the second through convection and radiation. The difference between the passive cooling method and the active cooling method happens in the last stage. The active cooling method uses machines to increase the convective transfer of heat. This could be done by using fans or by using methods to circulate liquids around the system. However as noted in 2.6.2 convection will happen if there is a temperature gradient.

3. SIMULATION METHOD

3.1   Transducer Design

The transducer being simulated in this thesis is shown in picture 3.1. On the top of the transducer there are two matching layers to limit reflection of acoustic waves from skin. After this there is a set of electrodes in contact with a which layer. The top electrode is ground and the bottom sends the signal to the which layer. This which layer is tuned to send out high frequency ultrasound. The next part is the heatsink of copper surrounded by two isolation layers. This copper layer is the main way for the cooling of the transducer. The next part of the transducer are a set of which layers with accompanying electrodes. The last part of the transducer is the backing.

The transducer is 150mm long and 42mm wide. The height of every layer in the transducer is given in figure 3.1
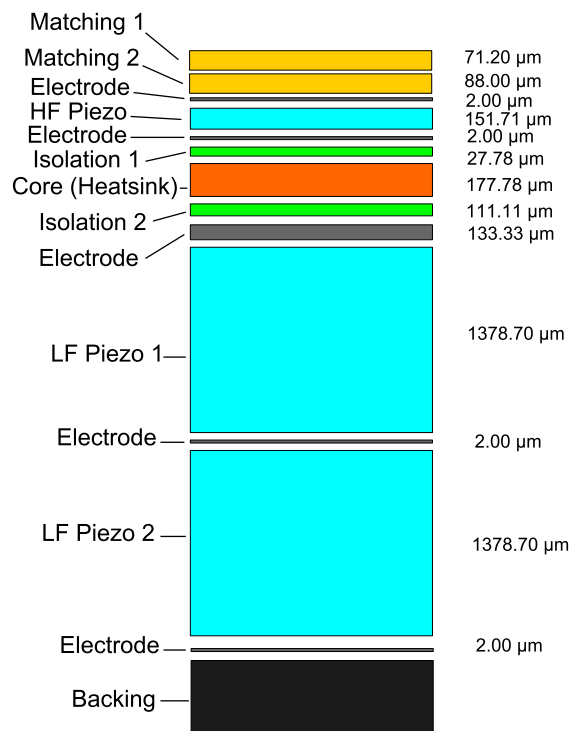
Fig. 3.1: Design of the transducer stack. The values on the right show the thickness of every layer.

3.2 COMSOL

The simulation program COMSOL Multiphysics is used in this thesis. The version used is 4.0a. COMSOL is a FEM program developed by COMSOL Inc. [3]. In order to use COMSOL one has to define the geometry, and material properties of the system to be simulated. Specify the initial conditions, the physical laws to be used.

3.2.1 Geometry
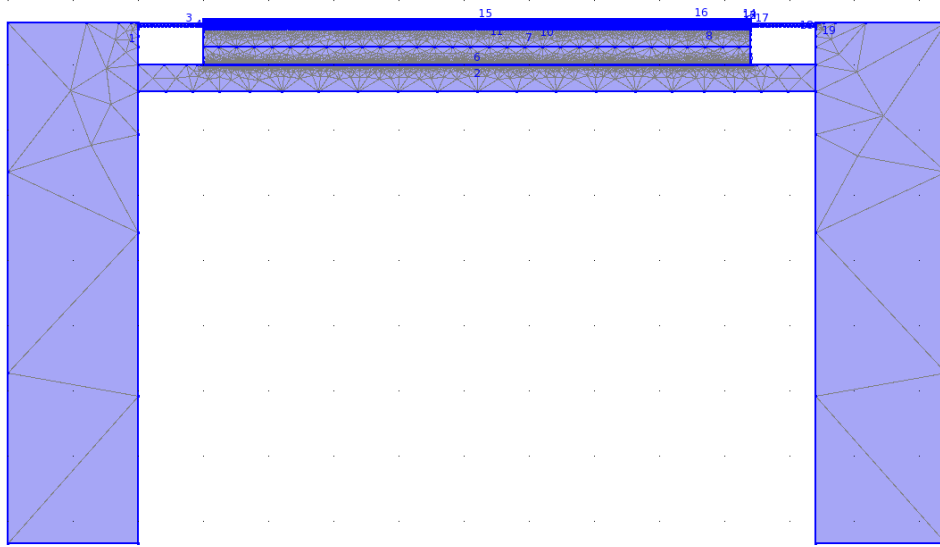
Fig. 3.2: Image showing the 2D geometry created in COMSOL. A mesh has been created to prepare for the simulation.
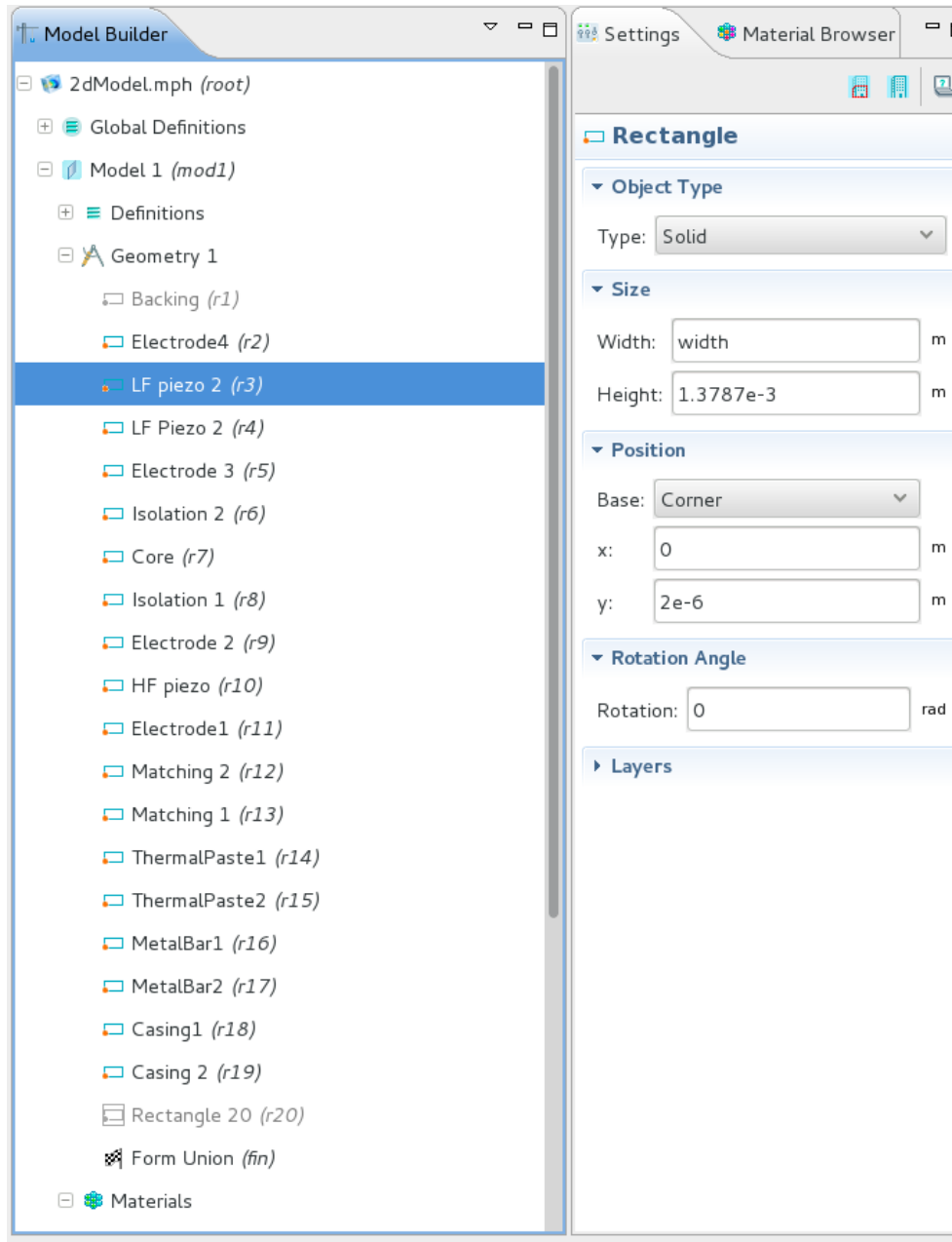
Fig. 3.3: Image showing the setup to create simulation geometry in COMSOL

3.2.2 Material

It is necessary in COMSOL to define the material parameters for the simulation. Figure 3.4 shows how this looks in COMSOL. The materials used for the simulations carried out in this thesis are further discussed in section 3.3.
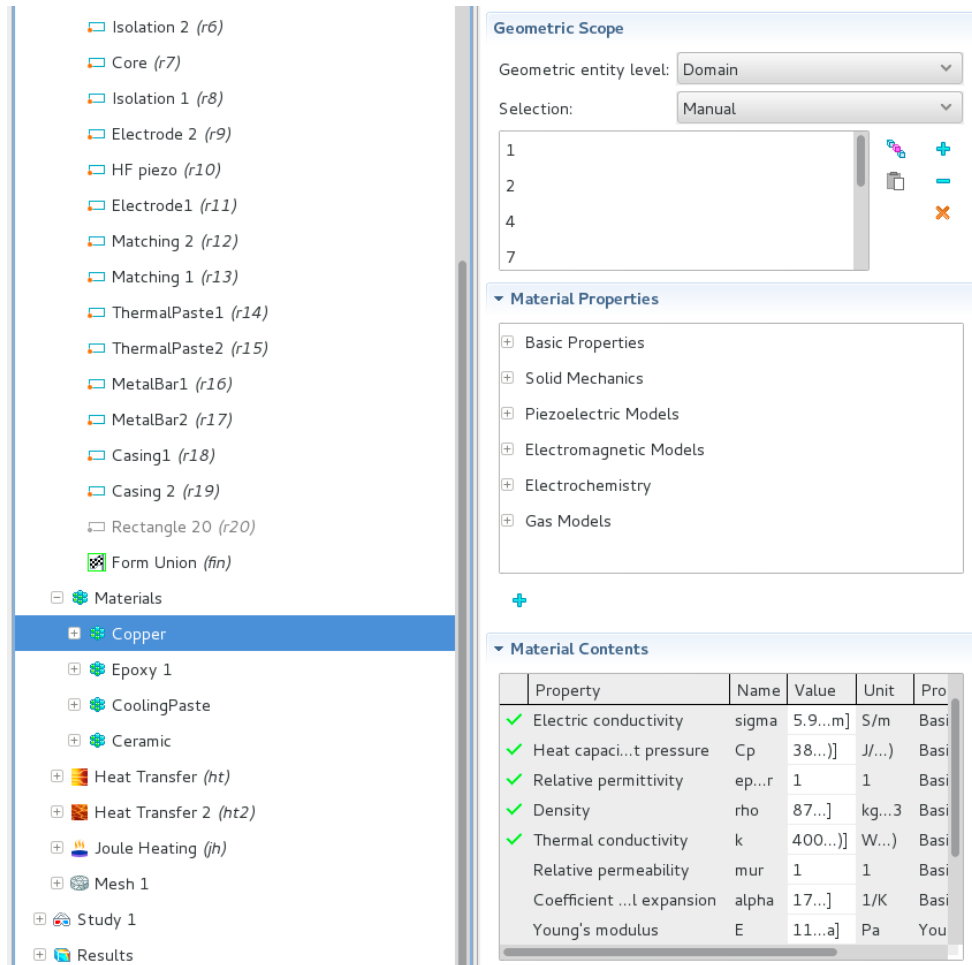
Fig. 3.4: Image showing the setup to define the material parameters in COMSOL

3.2.3   Initial Condition and physical laws

For the simulation to be successful it is necessary to define the physical laws to be used. These laws are the laws from section 2.6.1. It is also necessary to state the initial conditions. The initial conditions used in this thesis are starting temperature, border temperature and heat generation. The starting temperature was always set equal to the border temperature. The exact initial values vary depending on the simulations. They will be given along with the results.

3.3   Simulation Setup

The most accurate method of simulating heat transfer from the transducer, is to create a whole 3D model of the transducer. The downside of running a full 3D model of the transducer is that it increases the computational requirements. Running a simulation with the normal transducer layers, but with 4mm width and 4mm length, found that the simulation required 15mb of ram. This scale is small compared to the actual size of the transducer. 42mm width and 150mm length. A 3D model of the transducer, created in COMSOL, stack can be seen in figure 3.5

3DtransducerComsol.png

In the transducer from section 3.1 in a Cartesian coordinate system where the width is denoted as the x-dimension, the length is denoted as the y-dimension, and the height is denoted as the z-dimension. It is assumed that the heat generation inside the transducer is uniform in the different layers, the hottest point will be in the geometric center of the transducer as seen from above. Since finding the maximum temperature for a certain heat generation and geometry is the object of the simulation, this makes possible some simplifications of the simulation design. Instead of using a 3D model a 2D model can be used. The length of the transducer is 3.75 times its width. From 2.17 with the assumption of a uniform surface temperature $\frac{q_x}{A_x} = 3.75 \frac{q_y}{A_y}$ adding to this $A_x = 3.75 A_Y$. Therefore $q_x \approx 14 q_y$. The 2D simulation therefore as a first approximation only needs to take into account the x,z plane.

In order to simulate heat transfer from the transducer it was necessary to create the design to be simulated. Inside the transducer there are one or more copper plates whose task it is to transfer heat from the transducer to the outer casing. On the outer casing of the transducer there is an area of metal that exists in order to increase heat transfer between the casing and the surrounding air. The metal on the outer casing and the metal sheets in the transducer are attached. If these metal sheets were
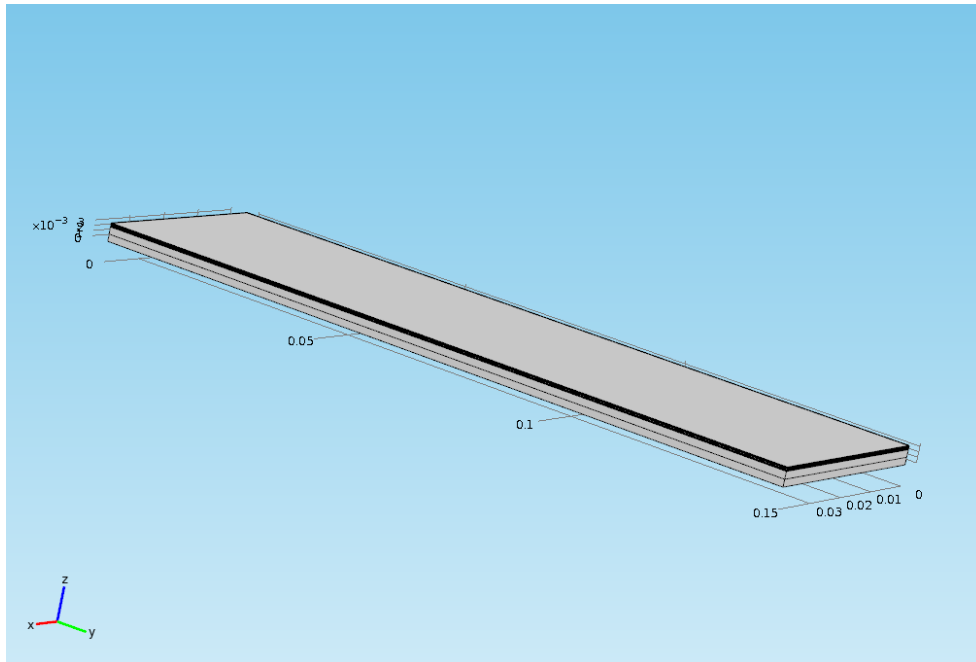
Fig. 3.5: Model of the transducer stack, created in COMSOL.

welded together this might change the stiffness of the apparatus, and lead to possible currents due to static electricity from the outside. Therefore these metal pieces are separated by a small layer of non-conductive thermal paste. This system can be seen in figure 3.6.

The simulation has been divided into two parts. Part 1 treats heat transfer from the casing to the surroundings. Part 2 treats heat transfer from the transducer to the casing. this is shown in figure 3.7

Part 1: Heat transfer from casing to the surroundings.

For the heat transfer from the casing to the surroundings. There are two mechanisms, free convection and radiation. Free convection is describe in section 2.6.2. Radiation is described in section 2.6.3. The simulation is conducted for several surface materials. These surface materials where: aluminum, anodized aluminum, polished copper, oxidized copper, copper painted black. The material parameters used are given in table 3.1
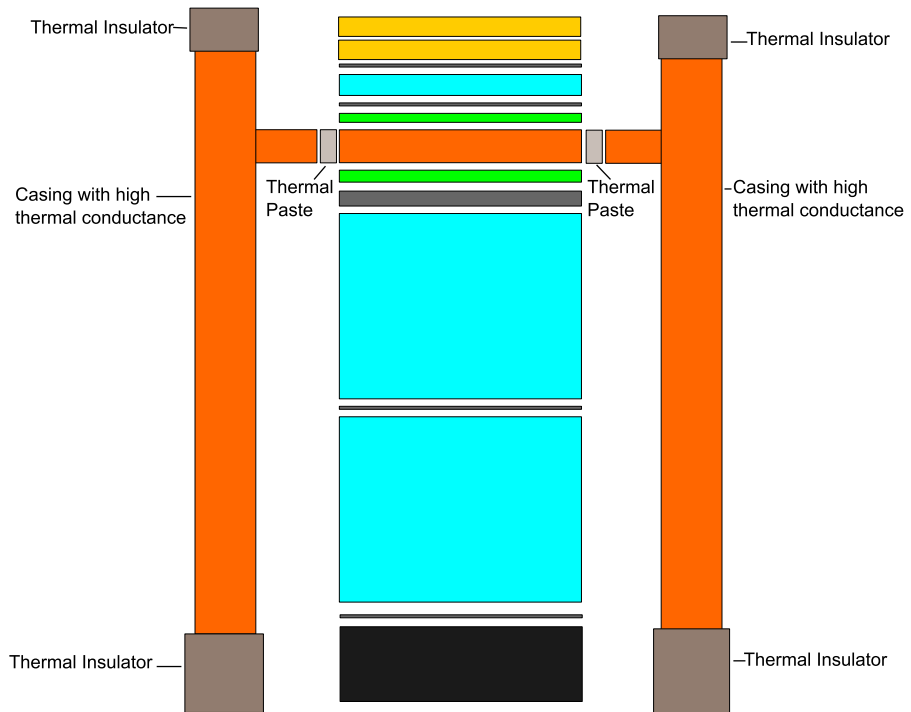
Fig. 3.6: System for cooling the transducer.

Overview of method

Part 1	• Calculation of heat transfer from casing to surroundings using functions in theory section and C#.
Part 2	• Simulation of heat transfer from transducer to casing using FEM in COMSOL.
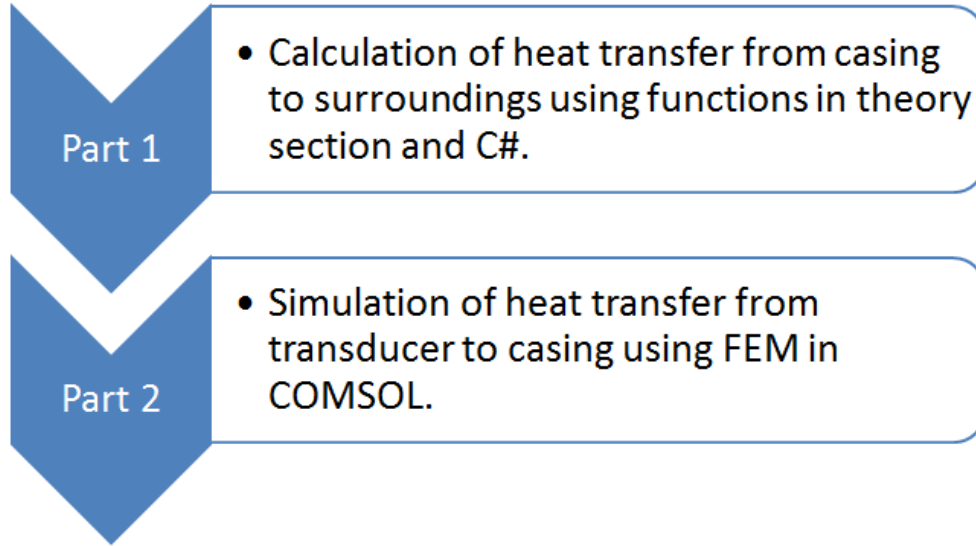
Fig. 3.7: The 2 part setup of the simulation.

Material	Heat Conductivity $[\frac{W}{m \cdot K}]$	Emissivity
aluminum	237	0.3
Anodized aluminum	237	0.84
Polished copper	401	0.07
Oxidized Copper	401	0.87
Copper Painted black	401	0.98

Tab. 3.1: Material properties used to simulate heat transfer from the casing to the surroundings. [17]

Material	$\rho \left[\frac{kg}{m^3}\right]$	$c_p \left[\frac{kJ}{kg \cdot K}\right]$	$\nu \left[\frac{m^2}{s}\right]$	k $\left[\frac{W}{m \cdot K}\right]$	$\alpha \left[\frac{m^2}{s}\right]$	Pr
Air	1.1614	1.007	$15.89 \cdot 10^{-6}$	$26.3 \cdot 10^{-3}$	$22.5 \cdot 10^{-6}$	0.707

Tab. 3.2: Air properties used to simulate heat transfer from the casing to the surroundings. [17]

Since radiation is an important part of heat transfer from the casing it is necessary to take into account the irradiation due to lighting on the casing. To investigate this

three cases will be used.

1. No lighting in the room.
This is equivalent $I = 0$ in equation 2.29 . This does not mean that the room has to be completely dark, it just means that the irradiation on the casing can be neglected.

2. Lighting equivalent to what is normal in an office environment. Offices have illuminance between 300 lux and 500 lux [2]. The amount of lumens/Watt ratio (also known as the Luminous efficacy of radiation) varies depending on the frequencies of the light. The maximum value is given at 555 nm (green light) at $683\frac{lm}{W}$ [29]. Light from a typical light bulb has a luminous efficacy of radiation of $15\frac{lm}{W}$, this is to a large part due to the radiation being in the infrared spectrum [25]. Sunlight has luminous efficacy of radiation of $93\frac{lm}{W}$ [25]. Light from LEDs have luminous efficacy of radiation around $60\frac{lm}{W}$ [25]. Some LEDs can however have higher efficiancy, [7] shows a 5.4W LED bulb, whose output is 410-550lm. This gives a wall-plug in luminous efficacy of $76 - 102\frac{lm}{W}$, since this efficency includes electricalloss the luminous efficacy of radiation will be even a bit higher. A conservative estimate of the Light in the room will then be $500lux/60\frac{lm}{W} \approx 8\frac{W}{m^2}$.

3. Direct sunLight hitting the transducer. At the surface of the earth, near the equator, the combined effect of direct sunLight and sunLight scattered from the athmosphere is $1120\frac{W}{m^2}$ [9]. This radiation changes quite a bit as you move away from the equator. It is however used as it gives an upper bound to the radiation incident in the transducer.

The heating caused by the incident Light varies a lot with the angle it hits the surface. For a grey surface the absorptivity does not change with the angle off the incident Light, the Light is however spread across a larger area if it hits at a low angle. Figure 3.8 shows Light incident on a surface with angle θ. The Irradiance of the Light is I_{in}. The Irradiance of the light as measured by the surface is I_{eff}. It is assumed that the surface is a grey surface. The only difference between I_{in} and I_{eff} is therefore the area the Light is spread over. From Figure 3.8 it is clear that

$$I_{eff} = I_{in} \cdot cos(\theta) \tag{3.1}$$

From 3.1 it is clear that as the angle of incidence θ goes to zero the effective irradiance I_{eff} becomes negligent.

During this simulation surface temperature was assumed constant. This assumption will be discussed further in section 5.1.2 based on the acquired data. The tables in chapter 4 showing the heat transferred from the casing to the surroundings also have a column labeled $\frac{Internal\ conduction}{q_{tot}}$. This is a measure of how strong the internal conduction of the surface is compared to the heat transfer to the surroundings. It is calculated the following way: There is assumed to be a 1K difference between the top of the casing and the bottom of the casing, the heat flow resulting from this is then calculated using the methods from section 2.6.1.

Part 2: Heat transfer, transducer to casing.

For the case where the generated heat in the transducer is equal to the heat transferred from the casing to the air, the temperature in the system will be constant. This static system is what is simulated in COMSOL. I.e., if the transducer generates a constant value $\dot{q}$ of heat, what will the temperature of the system be if left alone.

The simulation of the casing to air system finds the total amount of heat transferred from the casing to the air at a certain surface temperature. These result gives the initial condition for the internal simulation of the transducer. As the initial condition the whole transducer is set to the surface temperature used in the casing to air temperature. At the surface of the casing this temperature is set to be unchanged during the whole simulation. The amount of heat transferred by the casing to the air at this temperature is set to be equal to the heat generated in the transducer. The heat generation is assumed to be evenly distributed throughout the transducer. This value is divided by the total heat transfer to the surroundings. This fraction is therefore a measure of how much bigger the internal conduction would be, with a 1K temperature difference, to the heat transfer to the surroundings.

The generated heat is assumed to be evenly distributed throughout the transducer. Section 2.4 discusses how heat is generated in a transducer. The energy of a transducer is brought in by the electrodes. This electrical energy is then converted to acoustic energy in the which layers. It makes sense that a lot of the heat generated, will happen in this conversion. The which layers take up most of the space in the transducer. It is also known that absorption of acoustic energy in the other layers
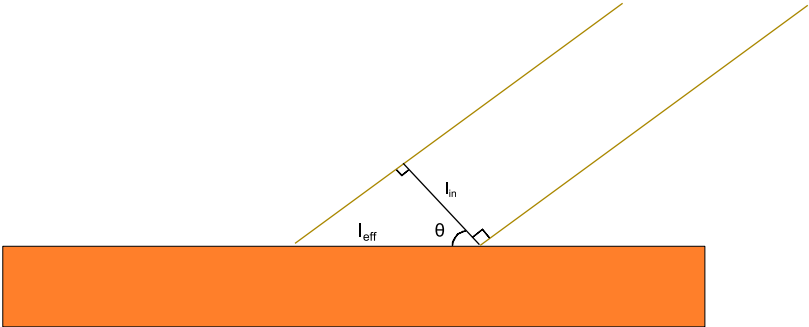
Fig. 3.8: Light incident on a surface at an angle. I_{in} is the Irradiance of the incoming light. I_{eff} is the effective irradiance after it has been spread out across the surface.

causes heat to be generated. The duty cycle of the which layers have not been determined. In equations 2.12 and 2.13 this is shown to be an important part of calculating the heat generation, and the distribution of the heat generation between the different which layers. Due to the unknown distribution of heat generation between the LF layer, the HF layers and the other layers, it was considered best to use assume the heat to be generated evenly throughout the transducer stack.

Materials

The simulation uses four groups of material parameters for the transducer stack. These materials are copper, epoxy, ceramic and thermal paste. Figure 3.5 shows the transducer stack

Copper is used for the electrodes , the core and the casing. COMSOL has already specified material values for copper. These values are:

- Density: $8700 \frac{kg}{m^3}$

- Specific heat capacity: $2100 \frac{J}{kg \cdot K}$

- Thermal conductivity: $0.18 - 3 \frac{W}{m \cdot K}$

Epoxy is used for the isolation layers and the matching layers. Epoxy is a relatively broad term, and refers to several materials. As the exact materials to be used for the isolation, matching layers where not clear, this general term was however used. [4] gives values in the following range for epoxies used in medical devices.

- Density: $1.02 - 1.25 \frac{kg}{m^3}$

- Specific heat capacity: $2100 \frac{J}{kg \cdot K}$

- Thermal conductivity: $0.18 - 3 \frac{W}{m \cdot K}$

The values that were used in the simulation are $\rho = 1.1 \frac{kg}{m^3}$, $c_P = 2100 \frac{J}{kg \cdot K}$, $k = 1 \frac{W}{m \cdot K}$.

Ceramic is used for the which layers. It was unknown exactly which materials were to be used in the transducer. $BaTiO_3$ is a ceramic material that has been used for transducers [5]. It is assumed that the piezoelectric layers are made of a material with

not very different properties from this. [23] gives the following values for $BaTiO_3$ based ceramics.

- Density: $(5.84 \pm 0.01) \cdot 10^3 \frac{kg}{m^3}$

- Specific heat capacity: $385 \pm 4 \frac{J}{kg \cdot K}$

- Thermal conductivity: $400 \pm 0.02 \frac{W}{m \cdot K}$

Thermal paste is used for the thermal paste section between the core and the casing. There are many different thermal pastes available. These are usually silicon based, with added materials to increase the thermal conductivity. Examples off added materials are, ceramics, metals such as aluminum and silver, and diamonds and other carbon based materials. The thermal paste T636 from Parker Chomerics has the following specifications, $\rho = 1.2 \frac{kg}{m^3}$, $c_P = 1200 \frac{J}{kg \cdot K}$, $k = 2.4 \frac{W}{m \cdot K}$ [6]. There are many thermal pastes with higher thermal conductivity as an example [8] has thermal conductivity of $k = 16 \frac{W}{m \cdot K}$. Thermal conductivity around $k = 10 \frac{W}{m \cdot K}$ is quite normal. The values chosen for the thermal paste material in the simulation are $\rho = 1.2 \frac{kg}{m^3}$, $c_P = 1200 \frac{J}{kg \cdot K}$, $k = 10 \frac{W}{m \cdot K}$.

4. RESULTS

4.0.1   Heat transfer from casing to surroundings.

The results in tables 4.1, 4.2, 4.3, 4.3, 4.4, 4.5,4.6, 4.7, 4.8, 4.9, 4.10, 4.11, 4.12, 4.13, 4.14, 4.15,where acquired for heat transfer between the cover and the surrounding air. Tables 4.1, 4.2, 4.3, 4.3, 4.4, 4.5,4.6, 4.7, 4.8, 4.9 are for casings with length 16cm, width 5.2cm and height 1cm.

T_S [C^o]	Ra_L	q_{conv} [W]	q_{rad} [W]	q_{tot} [W]	$\frac{Internal\ conduction}{q_{tot}}$
25	$4.65 \cdot 10^2$	0.171	0.0372	0.208	482
30	$9.21 \cdot 10^2$	0.392	0.0763	0.468	214
35	$1.37 \cdot 10^3$	0.637	0.117	0.755	133
40	$1.81 \cdot 10^3$	0.900	0.161	1.06	95
45	$2.25 \cdot 10^3$	1.18	0.206	1.38	73
50	$2.67 \cdot 10^3$	1.46	0.253	1.72	59
55	$3.10 \cdot 10^3$	1.76	0.303	2.07	49

Tab. 4.1: Heat transfer from casing to air for oxidized aluminium. No strong direct Lightsource. Casing with length 16cm, width 5.2cm and height 1cm.

T_S [C^o]	Ra_L	q_{conv} [W]	q_{rad} [W]	q_{tot} [W]	$\frac{Internal\ conduction}{q_{tot}}$
25	$4.65 \cdot 10^2$	0.171	0.104	0.275	365
30	$9.21 \cdot 10^2$	0.392	0.214	0.605	166
35	$1.37 \cdot 10^3$	0.637	0.329	0.966	104
40	$1.81 \cdot 10^3$	0.900	0.450	1.35	74
45	$2.25 \cdot 10^3$	1.18	0.577	1.75	57
50	$2.67 \cdot 10^3$	1.46	0.710	2.17	46
55	$3.10 \cdot 10^3$	1.76	0.849	2.61	38

Tab. 4.2: Heat transfer from casing to air for anodized aluminium. No strong direct Lightsource. Casing with length 16cm, width 5.2cm and height 1cm.

Tables 4.6, 4.7 are for ordinary office Light 8 $\frac{W}{m^2}$ on the cover.

Tables 4.8, 4.9, are for direct sun Light at strength 1100 $\frac{W}{m^2}$ on half of the cover.

T_S [C^o]	Ra_L	q_{conv} [W]	q_{rad} [W]	q_{tot} [W]	$\frac{Internal\ conduction}{q_{tot}}$
25	$4.65 \cdot 10^2$	0.171	0.00869	0.180	946
30	$99.21 \cdot 10^2$	0.392	0.0178	0.409	415
35	$1.37 \cdot 10^3$	0.637	0.0274	0.664	256
40	$1.81 \cdot 10^3$	0.900	0.0375	0.937	181
45	$2.25 \cdot 10^3$	1.18	0.0481	1.22	139
50	$2.67 \cdot 10^3$	1.46	0.0591	1.52	111
55	$3.10 \cdot 10^3$	1.76	0.0708	1.83	93

Tab. 4.3: Heat transfer from casing to air for polished copper. No strong direct Lightsource. Casing with length 16cm, width 5.2cm and height 1cm.

T_S [C^o]	Ra_L	q_{conv} [W]	q_{rad} [W]	q_{tot} [W]	$\frac{Internal\ conduction}{q_{tot}}$
25	$4.65 \cdot 10^2$	0.171	0.108	0.279	610
30	$9.21 \cdot 10^2$	0.392	0.221	0.613	277
35	$1.37 \cdot 10^3$	0.637	0.341	0.978	174
40	$1.81 \cdot 10^3$	0.900	0.466	1.365	125
45	$2.25 \cdot 10^3$	1.18	0.597	1.77	96
50	$2.67 \cdot 10^3$	1.46	0.735	2.20	77
55	$3.10 \cdot 10^3$	1.76	0.879	2.64	64

Tab. 4.4: Heat transfer from casing to air for oxidized copper. No strong direct Lightsource. Casing with length 16cm, width 5.2cm and height 1cm.

T_S [C^o]	Ra_L	q_{conv} [W]	q_{rad} [W]	q_{tot} [W]	$\frac{Internal\ conduction}{q_{tot}}$
25	$4.65 \cdot 10^2$	0.171	0.122	0.293	581
30	$9.21 \cdot 10^2$	0.392	0.249	0.641	265
35	$1.37 \cdot 10^3$	0.637	0.384	1.02	167
40	$1.81 \cdot 10^3$	0.900	0.525	1.42	119
45	$2.25 \cdot 10^3$	1.18	0.673	1.85	92
50	$2.67 \cdot 10^3$	1.46	0.828	2.29	74
55	$3.10 \cdot 10^3$	1.76	0.990	2.75	62

Tab. 4.5: Heat transfer from casing to air for copper painted black. No strong direct Lightsource. Casing with length 16cm, width 5.2cm and height 1cm.

T_S [C^o]	Ra_L	q_{conv} [W]	q_{rad} [W]	q_{tot} [W]	$\dfrac{Internal\ conduction}{q_{tot}}$
25	$4.65 \cdot 10^2$	0.171	0.0784	0.249	681
30	$9.21 \cdot 10^2$	0.392	0.192	0.584	291
35	$1.37 \cdot 10^3$	0.637	0.311	0.948	179
40	$1.81 \cdot 10^3$	0.900	0.436	1.34	127
45	$2.25 \cdot 10^3$	1.18	0.568	1.74	97
50	$2.67 \cdot 10^3$	1.46	0.706	2.17	78
55	$3.10 \cdot 10^3$	1.76	0.850	2.61	65

Tab. 4.6: Heat transfer from casing to air for oxidized copper, normal office Lighting. Casing with length 16cm, width 5.2cm and height 1cm.

T_S [C^o]	Ra_L	q_{conv} [W]	q_{rad} [W]	q_{tot} [W]	$\dfrac{Internal\ conduction}{q_{tot}}$
25	$4.65 \cdot 10^2$	0.171	0.0883	0.259	656
30	$9.21 \cdot 10^2$	0.392	0.216	0.608	280
35	$1.37 \cdot 10^3$	0.637	0.351	0.986	172
40	$1.81 \cdot 10^3$	0.900	0.492	1.39	122
45	$2.25 \cdot 10^3$	1.18	0.640	1.82	94
50	$2.67 \cdot 10^3$	1.46	0.795	2.26	75
55	$3.10 \cdot 10^3$	1.76	0.957	2.72	63

Tab. 4.7: Heat transfer from casing to air for copper painted black, normal office Lighting. Casing with length 16cm, width 5.2cm and height 1cm.

T_S [C^o]	Ra_L	q_{conv} [W]	q_{rad} [W]	q_{tot} [W]	$\dfrac{Internal\ conduction}{q_{tot}}$
25	$4.65 \cdot 10^2$	0.171	-1.96	-1.79	-95
30	$9.21 \cdot 10^2$	0.392	-1.84	-1.45	-117
35	$1.37 \cdot 10^3$	0.637	-1.72	-1.09	-156
40	$1.81 \cdot 10^3$	0.900	-1.60	-0.70	-243
45	$2.25 \cdot 10^3$	1.18	-1.47	-0.292	-582
50	$2.67 \cdot 10^3$	1.46	-1.33	0.133	1276
55	$3.10 \cdot 10^3$	1.76	-1.19	0.576	295

Tab. 4.8: Heat transfer from casing to air for oxidized copper, under direct sunLight. Casing with length 16cm, width 5.2cm and height 1cm.

$T_S \ [C^o]$	Ra_L	q_{conv} [W]	q_{rad} [W]	q_{tot} [W]	$\frac{Internal\ conduction}{q_{tot}}$
25	$4.65 \cdot 10^2$	0.171	-2.21	-2.03	-84
30	$9.21 \cdot 10^2$	0.392	-2.08	-1.69	-101
35	$1.37 \cdot 10^3$	0.637	-1.94	-1.31	-130
40	$1.81 \cdot 10^3$	0.900	-1.80	-0.903	-188
45	$2.25 \cdot 10^3$	1.18	-1.65	-0.478	-356
50	$2.67 \cdot 10^3$	1.46	-1.50	-0.035	-4852
55	$3.10 \cdot 10^3$	1.76	-1.34	0.426	399

Tab. 4.9: Heat transfer from casing to air for copper painted black, under direct sunLight. Casing with length 16cm, width 5.2cm and height 1cm.

From now on all the tables will be for copper oxide or copper painted black under office Lighting. Tables 4.10, 4.11, are for casings with length 16cm, width 5.2cm and height 2cm.

T_S [C^o]	Ra_L	q_{conv} [W]	q_{rad} [W]	q_{tot} [W]	$\frac{Internal\ conduction}{q_{tot}}$
25	$3.72 \cdot 10^3$	0.262	0.157	0.417	203
30	$7.37 \cdot 10^3$	0.607	0.384	0.991	86
35	$1.10 \cdot 10^4$	0.994	0.622	1.62	53
40	$1.45 \cdot 10^4$	1.41	0.873	2.28	37
45	$1.80 \cdot 10^4$	1.85	1.14	2.98	28
50	$2.14 \cdot 10^4$	2.31	1.41	3.72	23
55	$2.48 \cdot 10^4$	2.78	1.70	4.48	19

Tab. 4.10: Heat transfer from casing to air for oxidized copper, normal office Lighting. Casing with length 16cm, width 5.2cm and height 2cm.

T_S [C^o]	Ra_L	q_{conv} [W]	q_{rad} [W]	q_{tot} [W]	$\frac{Internal\ conduction}{q_{tot}}$
25	$3.72 \cdot 10^3$	0.262	0.177	0.438	194
30	$7.37 \cdot 10^3$	0.607	0.432	1.04	82
35	$1.10 \cdot 10^4$	0.994	0.701	1.69	50
40	$1.45 \cdot 10^4$	1.41	0.983	2.39	36
45	$1.80 \cdot 10^4$	1.85	1.28	3.13	27
50	$2.14 \cdot 10^4$	2.31	1.59	3.90	22
55	$2.48 \cdot 10^4$	2.78	1.91	4.70	18

Tab. 4.11: Heat transfer from casing to air for copper painted black, normal office Lighting. Casing with length 16cm, width 5.2cm and height 2cm.

Tables 4.12, 4.13 are for casings with length 16cm, width 5.2cm and height 4cm.

T_S [C^o]	Ra_L	q_{conv} [W]	q_{rad} [W]	q_{tot} [W]	$\frac{Internal\ conduction}{q_{tot}}$
25	$2.97 \cdot 10^4$	0.414	0.314	0.728	58
30	$5.89 \cdot 10^4$	0.967	0.768	1.74	24
35	$8.78 \cdot 10^4$	1.59	1.24	2.84	15
40	$1.16 \cdot 10^5$	2.27	1.75	4.01	11
45	$1.44 \cdot 10^5$	2.98	2.27	5.25	8.1
50	$1.71 \cdot 10^5$	3.72	2.82	6.55	6.4
55	$1.98 \cdot 10^5$	4.50	3.40	7.90	5.4

Tab. 4.12: Heat transfer from casing to air for oxidized copper, normal office Lighting. Casing with length 16cm, width 5.2cm and height 4cm.

T_S [C^o]	Ra_L	q_{conv} [W]	q_{rad} [W]	q_{tot} [W]	$\frac{Internal\ conduction}{q_{tot}}$
25	$2.97 \cdot 10^4$	0.414	0.353	0.768	55
30	$5.89 \cdot 10^4$	0.967	0.865	1.83	23
35	$8.78 \cdot 10^4$	1.59	1.40	3.00	14
40	$1.16 \cdot 10^5$	2.27	1.97	4.23	10
45	$1.44 \cdot 10^5$	2.98	2.56	5.54	7.7
50	$1.71 \cdot 10^5$	3.72	3.18	6.90	6.2
55	$1.98 \cdot 10^5$	4.50	3.83	8.33	5.1

Tab. 4.13: Heat transfer from casing to air for copper painted black, normal office Lighting. Casing with length 16cm, width 5.2cm and height 4cm.

Tables 4.14, 4.15 are for casings with length 16cm, width 5.2cm and height 8cm.

T_S [C^o]	Ra_L	q_{conv} [W]	q_{rad} [W]	q_{tot} [W]	$\frac{Internal\ conduction}{q_{tot}}$
25	$2.81 \cdot 10^5$	0.671	0.627	1.30	16
30	$4.71 \cdot 10^5$	1.58	1.54	3.11	6.8
35	$7.02 \cdot 10^5$	2.60	2.49	5.09	4.2
40	$9.27 \cdot 10^6$	3.71	3.49	7.20	2.9
45	$1.15 \cdot 10^7$	4.88	4.54	9.42	2.3
50	$1.37 \cdot 10^7$	6.11	5.64	11.8	1.8
55	$1.59 \cdot 10^7$	7.38	6.80	14.2	1.5

Tab. 4.14: Heat transfer from casing to air for oxidized copper, normal office Lighting. Casing with length 16cm, width 5.2cm and height 8cm.

T_S [C^o]	Ra_L	q_{conv} [W]	q_{rad} [W]	q_{tot} [W]	$\frac{Internal\ conduction}{q_{tot}}$
25	$2.81 \cdot 10^5$	0.671	0.701	1.38	15
30	$4.71 \cdot 10^5$	1.58	1.73	3.31	6.4
35	$7.02 \cdot 10^5$	2.60	2.80	5.41	3.9
40	$9.27 \cdot 10^6$	3.71	3.93	7.64	2.8
45	$1.15 \cdot 10^7$	4.88	5.12	10.0	2.1
50	$1.37 \cdot 10^7$	6.11	6.36	12.5	1.7
55	$1.59 \cdot 10^7$	7.38	7.66	15.0	1.4

Tab. 4.15: Heat transfer from casing to air for copper painted black, normal office Lighting. Casing with length 16cm, width 5.2cm and height 8cm.

The highest amount of heat transferred to the surroundings was 15.0W for a casing of height 8cm made out of copper painted black at surface temperature of $55C^o$. This result however has a $\frac{Internal\ conduction}{q_{tot}}$ of only 1.4, it is therefore unlikely that the surface temperature is constant. It is clear that the bigger the cover is the more heat is transferred. It is also clear that the material has a big impact on the heat transfer, especially for radiation.

4.0.2 Internal heat transfer.

This section presents results for simulations of heat transfer internally in the transducer. In all simulations the surface temperature of the transducer is held at constant ant there is an evenly distributed heat generation in the transducer stack. The parameters for heat generation and surface temperature are taken from table 4.13. All simulations are therefore of a system with a copper casing if 4cm height painted black. The casing temperatures range from 40 C^o to 55 C^o. The simulations show the impact of different thicknesses of thermal paste. They show the distribution of heat in the transducer stack. Figure 4.9 show the added heat transfer due to an extra copper layer at the bottom of the transducer stack.

Figures 4.1 and 4.2 show the static temperature distribution for a casing boundary of $T_S = 40C^o$, and an evenly distributed heat generation of 4.23W. Both show the transducer in the hight-width plane. The difference between the two simulations is that 4.1 has a thermal paste layer if 0.1 mm, and 4.2 has a thermal paste layer if 0.1 mm. For both simulations the warmest point is found at the center of the bottom of the transducer stack. The highest temperature for 4.1 is $43.25C^o$, 3.25 C^o above T_S, and for 4.2 it is $50.25C^o$,10.25 C^o above T_S.

Surface: Temperature (K)
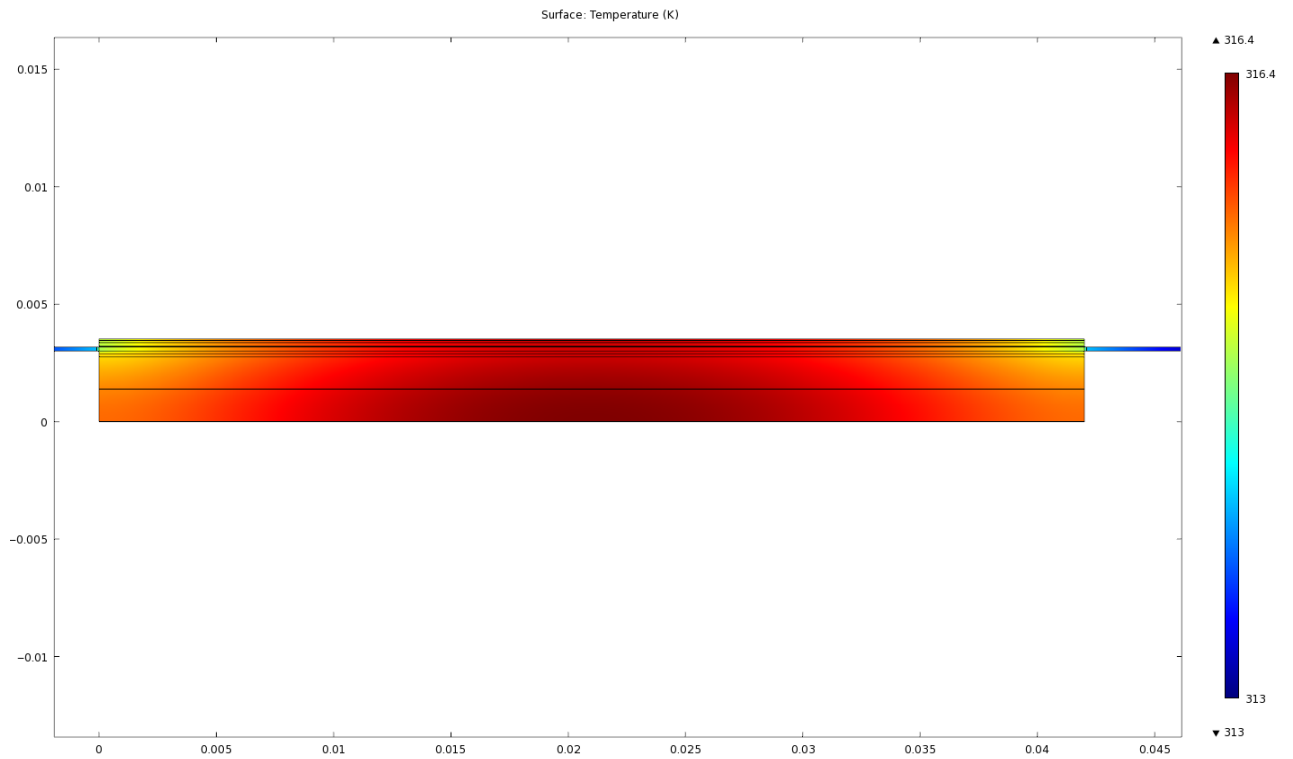
Fig. 4.1: The static temperature distribution for a casing boundary of $40C^o$, and an evenly distributed heat generation of 4.23W. The thermal paste is 0.1mm thick. The maximum temperature is $43.25C^o$.
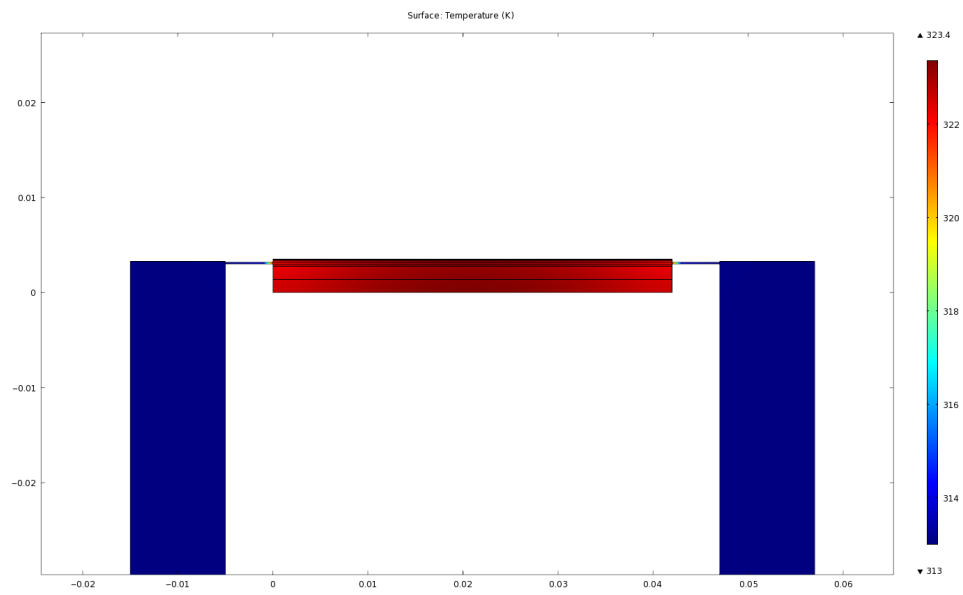
Fig. 4.2: The static temperature distribution for a casing boundary of $40C^o$, and an evenly distributed heat generation of 4.23W. The thermal paste is 1mm thick. The maximum temperature is $50.25C^o$.

Figures 4.3 and 4.4 show the static temperature distribution for a casing boundary of $T_S = 45C^o$, and an evenly distributed heat generation of 5.54W. Both show the transducer in the hight-width plane. The difference between the two simulations is that 4.3 has a thermal paste layer if 0.1 mm, and 4.4 has a thermal paste layer if 0.1 mm. For both simulations the warmest point is found at the center of the bottom of the transducer stack. The highest temperature for 4.3 is $49.35C^o$, 4.45 C^o above T_S, and for 4.4 it is $58.45C^o$, 13.45 C^o above T_S.
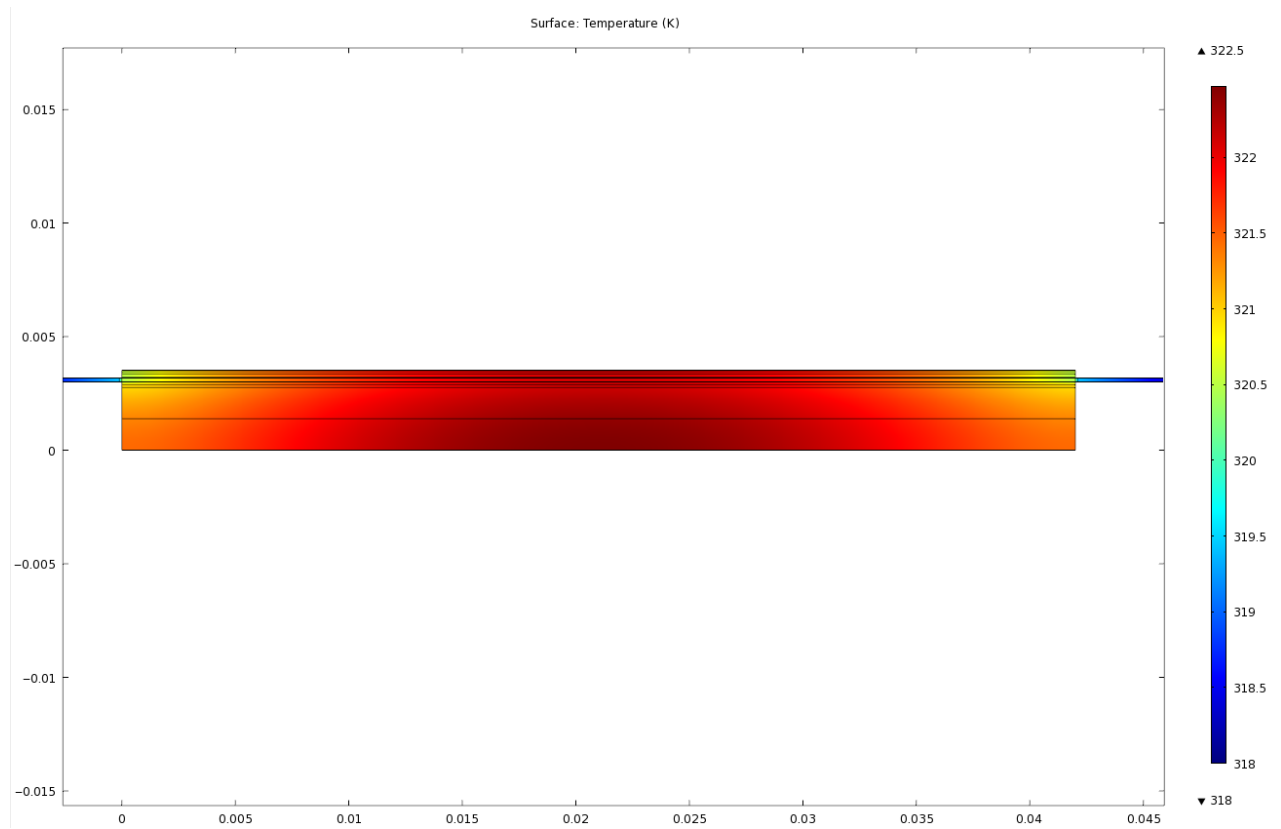
Fig. 4.3: The static temperature distribution for a casing boundary of $45C^o$, and an evenly distributed heat generation of 5.54W. The thermal paste is 0.1mm thick. The maximum temperature is $49.35C^o$.
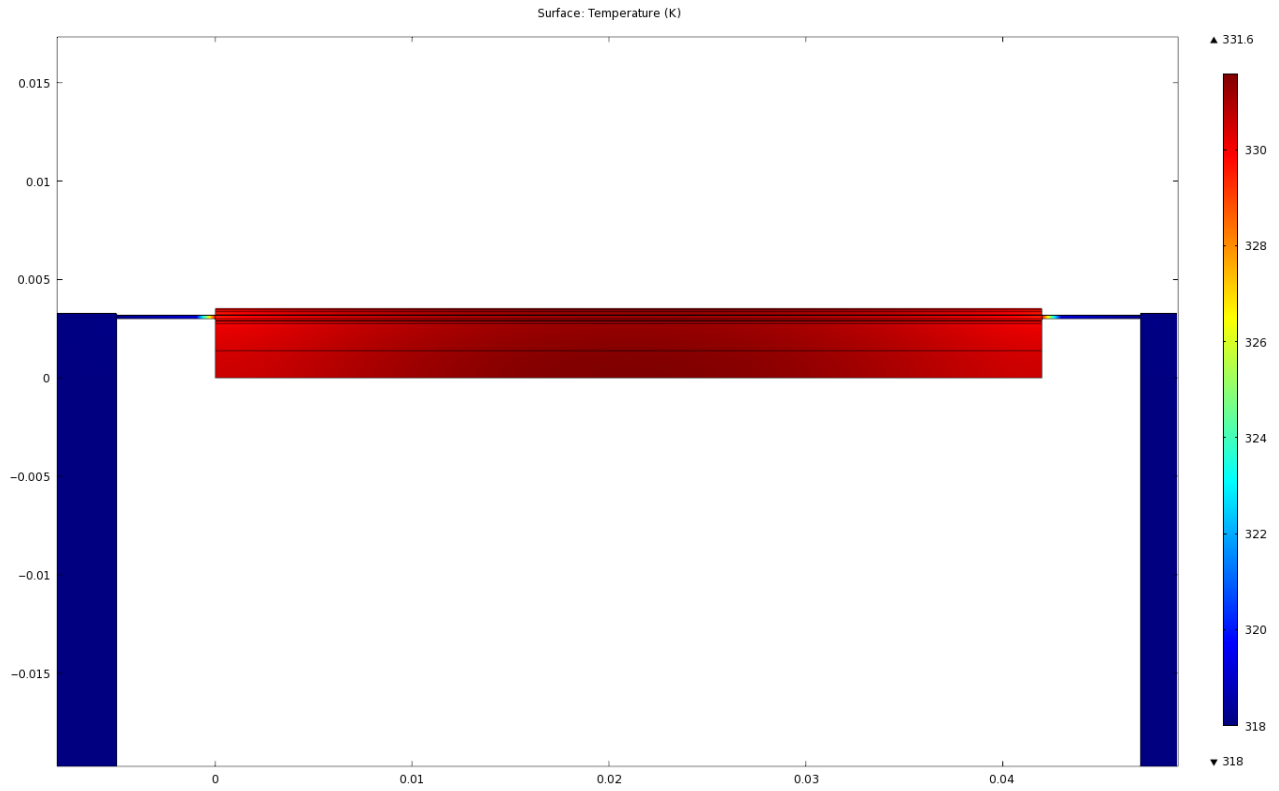
Fig. 4.4: The static temperature distribution for a casing boundary of $45C^o$, and an evenly distributed heat generation of 5.54W. The thermal paste is 1mm thick. The maximum temperature is $58.45C^o$.

Figures 4.5 and 4.6 show the static temperature distribution for a casing boundary of $T_S = 50C^o$, and an evenly distributed heat generation of 6.90W. Both show the transducer in the hight-width plane. The difference between the two simulations is that 4.5 has a thermal paste layer if 0.1 mm, and 4.6 has a thermal paste layer if 0.1 mm. For both simulations the warmest point is found at the center of the bottom of the transducer stack. The highest temperature for 4.5 is $55.45C^o$,5.45 C^o above T_S, and for 4.6 it is $66.75C^o$, ,16.75 C^o above T_S,.

Surface: Temperature (K)
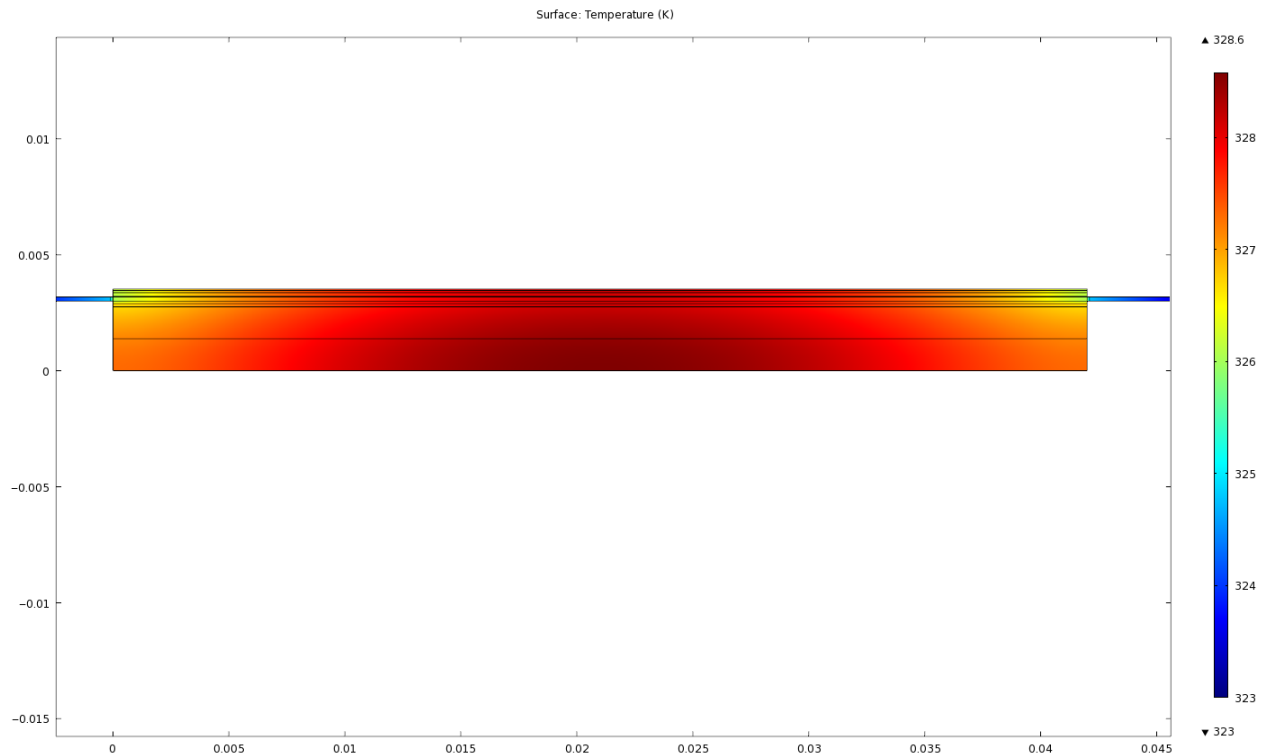
Fig. 4.5: The static temperature distribution for a casing boundary of $50C^o$, and an evenly distributed heat generation of 6.90W. The thermal paste is 0.1mm thick. The maximum temperature is $55.45C^o$.
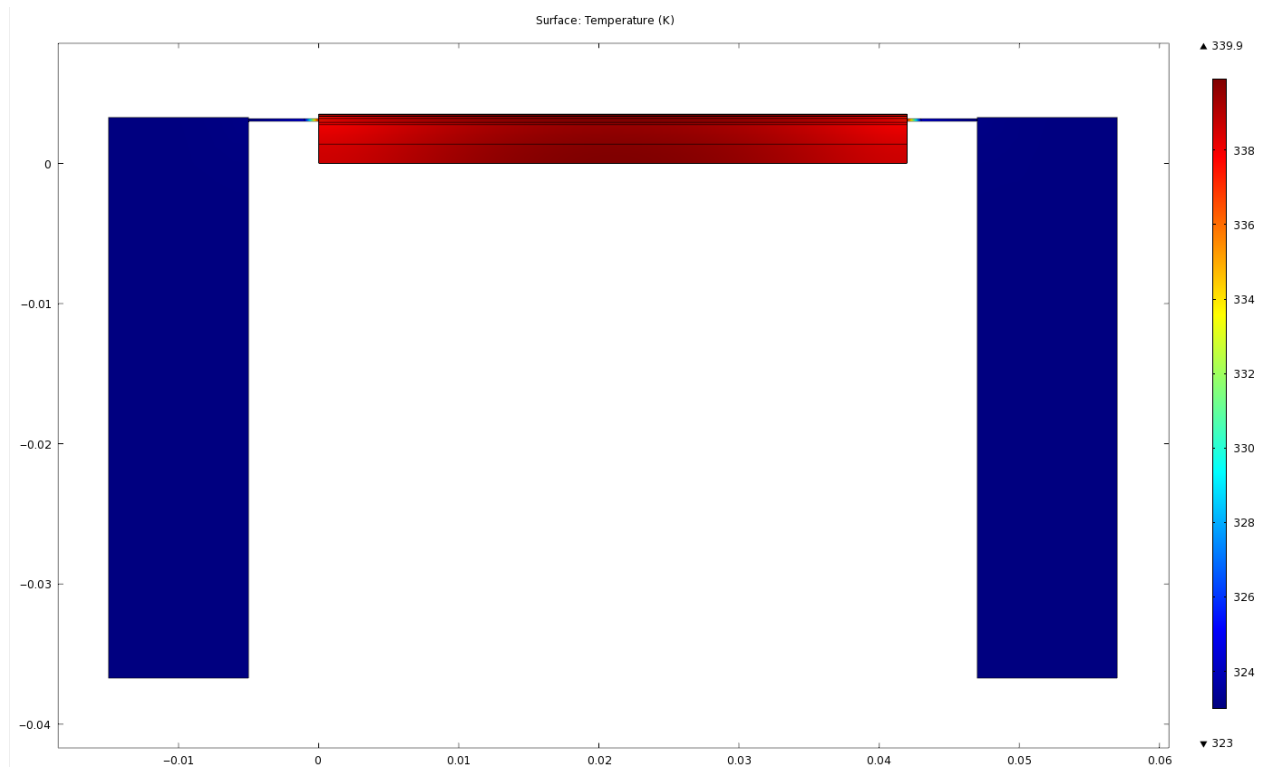
Fig. 4.6: The static temperature distribution for a casing boundary of $50C^o$, and an evenly distributed heat generation of 6.90W. The thermal paste is 1mm thick. The maximum temperature is $66.75C^o$.

Figures 4.7 and 4.8 show the static temperature distribution for a casing boundary of $T_S = 55C^o$, and an evenly distributed heat generation of 8.33W. Both show the transducer in the hight-width plane. The difference between the two simulations is that 4.7 has a thermal paste layer if 0.1 mm, and 4.8 has a thermal paste layer if 0.1 mm. For both simulations the warmest point is found at the center of the bottom of the transducer stack. The highest temperature for 4.7 is $61.55C^o$,6.55 C^o above T_S, and for 4.8 it is $75.25C^o$,20.25 C^o above T_S.
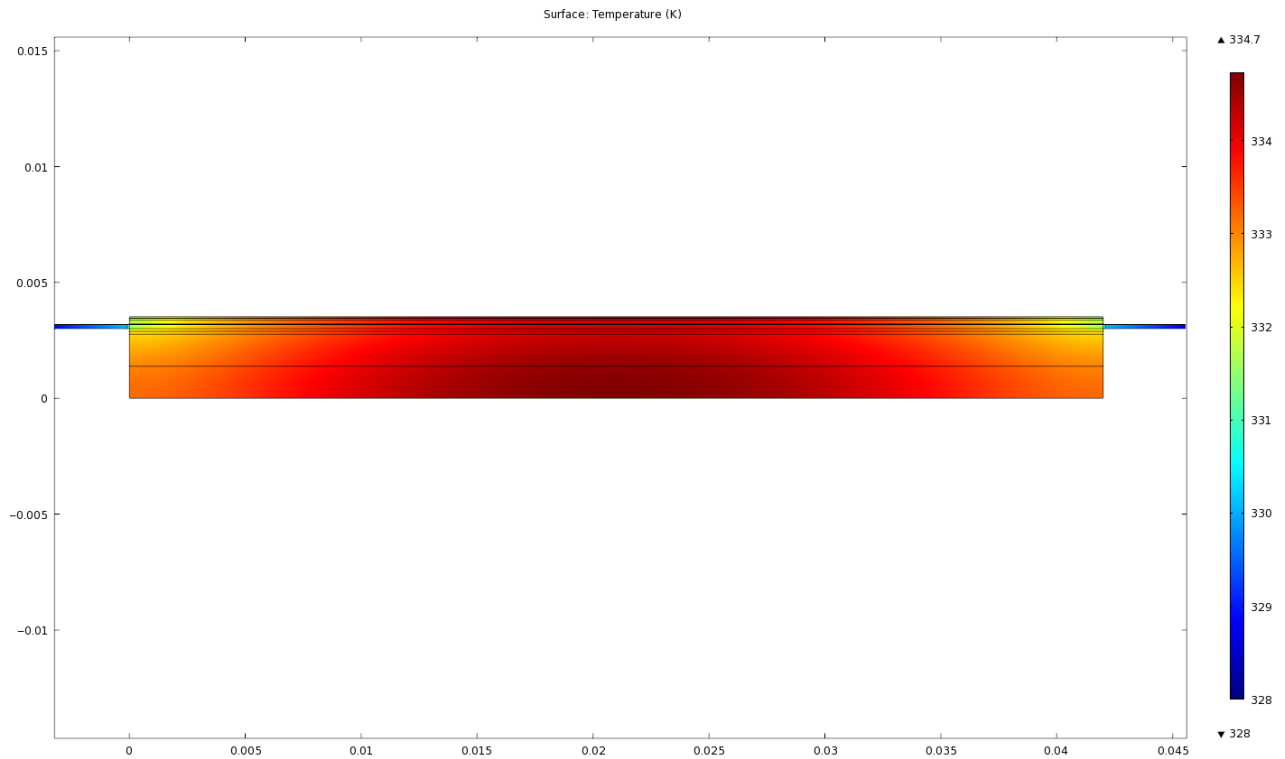
Fig. 4.7: The static temperature distribution for a casing boundary of $55C^o$, and an evenly distributed heat generation of 8.33W. The thermal paste is 0.1mm thick. The maximum temperature is $61.55C^o$.
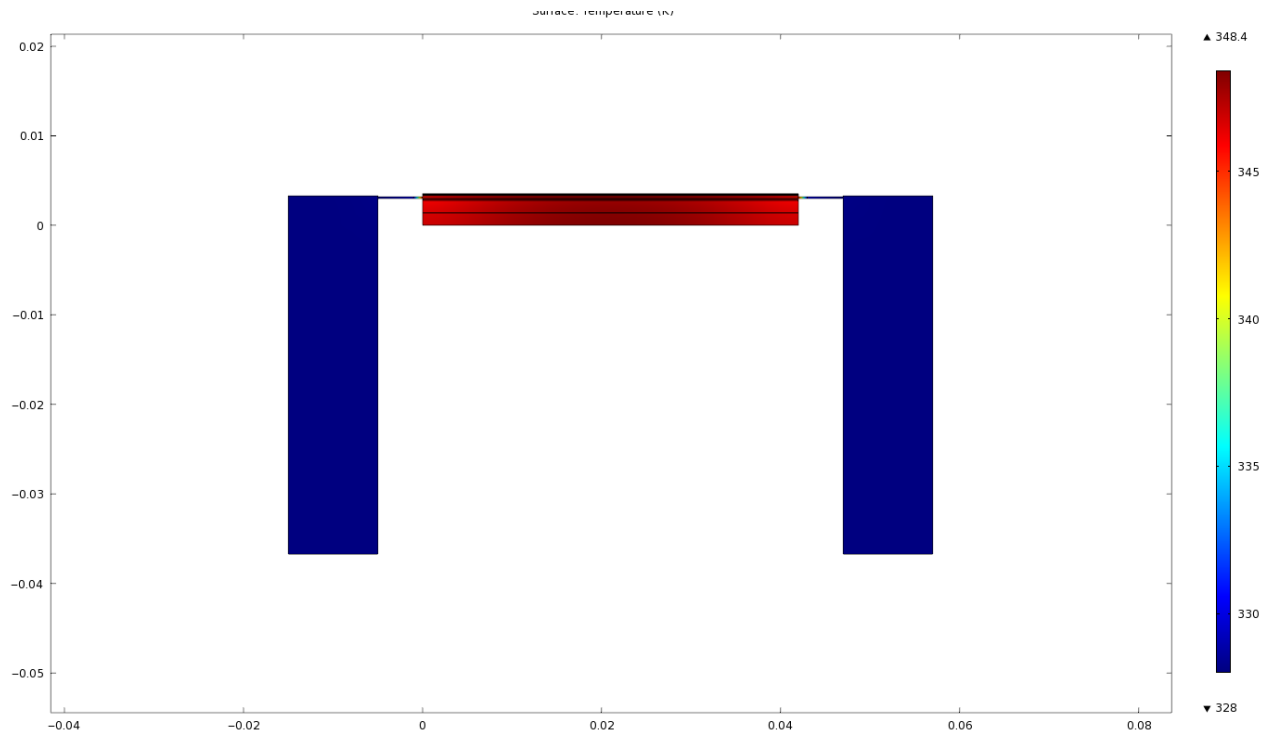
Fig. 4.8: The static temperature distribution for a casing boundary of $55C^o$, and an evenly distributed heat generation of 8.33W. The thermal paste is 1mm thick. The maximum temperature is $75.25C^o$.

In figures 4.1, 4.2, 4.3, 4.4, 4.5, 4.6, 4.7, 4.8 the hottest point is at the bottom of the transducer stack. For this reason a simulation was run to determine the effect of an added heat conducting layer at the bottom of the transducer. This simulation is shown in figure 4.9. The material of this new layer is copper, the thickness of this layer is 2mm. The casing temperature is $T_S = 55C^o$, the evenly distributed heat generation is 8.33W, the thickness of the thermal paste is 1mm. Except for the new conductive layer, this is the same simulation as shown in figure 4.8. Figure reffig:TempDist9 show that with the added conductive layer the hottest point is at the top of the transducer and has a temperature of $56.15C^o$, only 1.15 C^o above the temperature of the casing.
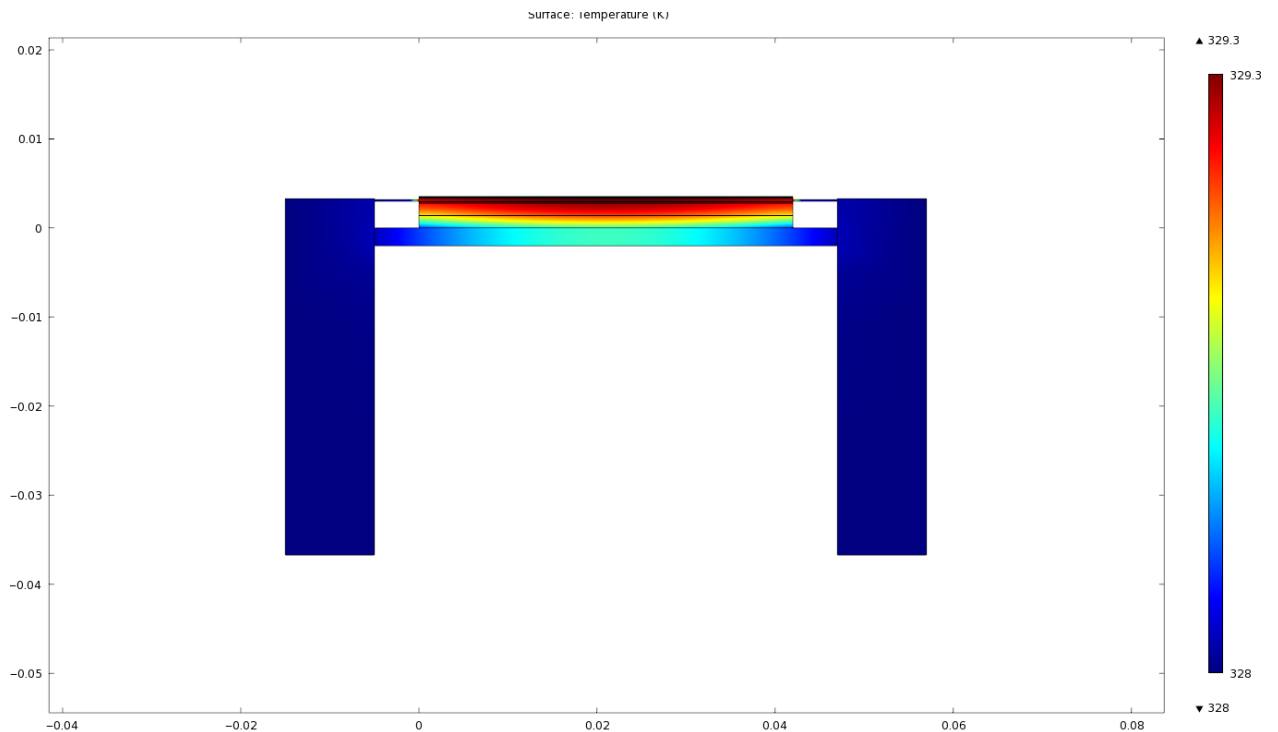
Fig. 4.9: The static temperature distribution for a casing boundary of $55C^o$, and an evenly distributed heat generation of 8.33W. The thermal paste is 1mm thick. In addition to the cooling from the core, there is also cooling from the added bar under the transducer stack. This bar is assumed to be of copper. The maximum temperature is $56.15C^o$.

Figure 4.16 shows the maximum temperatures from figures 4.1, 4.2, 4.3, 4.4, 4.5, 4.6, 4.7, 4.8. It displays the simulation using the same casing temperature and heat generation next to each other. The difference in the maximal temperatures is also shown.

T_S	Maximal temperature, thermal paste: 0.1mm	Maximal temperature, thermal paste: 1mm	Differenc
40 C^o	43.25C^o	50.25C^o	
45 C^o	49.35C^o	58.45C^o	
50 C^o	55.45C^o	66.75C^o	
55 C^o	61.55C^o	75.25C^o	

Tab. 4.16: Maximum temperatures for simulations made with varying thickness of thermal paste.

5. DISCUSSION

5.1 Casing to surroundings

5.1.1 Lighting

As the values presented in tables 4.4, 4.5, 4.6, 4.7, 4.8 and 4.9 it is clear that the Light on the transducer can have a large effect. Tables 4.8 and 4.9 show that under strong direct sunLight the heat transfer might actually be negative. This means that the casing leads heat into the transducer stack instead of out of the transducer stack. Comparing tables 4.7 and 4.5 show that the difference from no incident Light on the transducer, and normal office Lighting is not big. For a surface temperature of $55C^o$ the heat flux is 2.72W under normal office Lighting and 2.75W without lighting.

If a cooling mechanism as proposed in this thesis is to be used it is necessary to avoid strong Light on the transducer. It is especially important to block strong light that comes normal to the casing. As shown in equation 3.1 Light hitting the surface at a steep angle results in much less heating than Light hitting the surface at close to a normal angle. In strong Lighting conditions it is therefore be possible to greatly reduce the heating effects caused by the strong light, by placing a shield blocking the strongest most direct Light on the casing.

5.1.2 Material

Tables 4.1, 4.2, 4.3, 4.4 and 4.5 show the cooling effect of different casing materials with different surface coatings. The results show that the material properties of the casing does not influence the convective heat transfer. Section 2.6.2 also show this as the material properties of the surface are not part of the equations. Instead the convection only depends on the temperature of the surface, the area of the surface, the material properties of the fluid surrounding the surface and the movement of this

fluid. This is however a simplification. In the calculation for convection it is assumed that the temperature of the surface is constant. If the conductivity off the surface material is low compared to the heat flow from the surface to the environment this assumption will be false. Parts of the surface in this case do not participate much in the heat transfer from surface to surroundings since these parts will be cooled down quite a bit. The end result of a thermal conductive material is to limit the amount of heat that can be transferred to the surroundings. This is measured by the last column in the table.

Comparing the tables 4.1, 4.2, 4.3, 4.4 and 4.5 with the material values given in table 3.1 show the importance of a high emissivity in order to increase radiative heat transfer. For a surface of $55C^o$ polished copper has a radiative heat transfer of 0.708W, whereas copper painted black has a radiative heat transfer of 0.990. This is as expected from equation 2.29.

There is a very clear increase of heat transfer with surface temperature. Equation 2.29 gives $q_{rad} \propto T_S^4$. Equation 2.19 makes it seem that $q_{conv} \propto T_S$, however it also gives $q_{conv} \propto h$. Equation 2.20 gives that $\bar{h} \propto \bar{Nu}_L$, equation 2.21 gives $\bar{Nu}_L \propto Ra_L^{\frac{1}{4}}$, and equation 2.23 gives $Ra_L \propto T_S$. The end result is that $q_{conv} \propto T_S \cdot T_S^{\frac{1}{4}} = T_S^{\frac{5}{4}}$.

It is clear from sections 5.1.1 and 5.1.2 that the ideal casing material has high conductivity and high emissivity. From the materials in table 3.1 copper painted black is the best material. This is the reason why this material is the only one used i subsequent tables. The second best material is oxidized copper, due to its high conductivty. That copper was the best material used here does not mean that there aren't better material available.

5.1.3   Size of conductive casing

The heat transfer varies a lot with the size of the conductive casing area. Tables 4.13 and 4.14 show that with an increase in the height of the conductive area from 4cm to 8 cm the heat transferred, for $T_S = 55C^o$ goes from 8.33W to 15.0W. In general when the height of this area is doubled the heat transferred is close to doubled. For the case of a height of 8cm the ratio of internal conduction to heat transferred to the surroundings is only 1.4. This shows that the assumption of constant surface tem-

perature is unlikely to be true. The heat transferred to the surroundings is therefore likely to be less than 15W. 8cm height is quite a large area for a medical transducer. Especially since this area should ideally not be touched. The conductive area of 4cm is what has been used for the internal simulations using COMSOL.

5.2   Conduction inside the transducer

The simulations 4.1, 4.2, 4.3, 4.4, 4.5, 4.6, 4.7, 4.8 show that there is a large increase in the maximum temperature of the transducer for the simulation with thermal paste of 1mm compared to the ones with thermal paste 0.1mm. This is an important result to be aware off. since it means one have to be very precise when applying the cooling paste. Variations in the thickness of the cooling paste will mean that one can not be certain of the internal temperature of the transducer just based on the surface temperature of the casing and the heat generation. Due to this uncertainty it would be useful to have a temperature sensor in the transducer to avoid overheating. The bottom of the transducer stack seems a good place to place such a sensor.

In the simulations 4.1, 4.2, 4.3, 4.4, 4.5, 4.6, 4.7, 4.8 the warmest point is always the bottom of the first piezoelectric layer. This is due to this point being furthest away from the copper core. A simulation was done to test the result of adding a copper layer beneath the transducer stack, this simulation is shown in 4.8. This simulation was done with $T_S = 55C^o$, the heat generation was 8.33W and the thermal paste layer was 1mm. The maximum temperature in the transducer stack was $56.15C^o$ only $1.15C^o$ higher than T_S. Except for the new copper layer the simulation parameters are exactly the same as in 4.8 where the maximum temperature was $75.25C^o$,20.25 C^o above T_S. The temperature gradient with the new conductive layer is only 1.15/20.25= 5.7

Improvements to the heat transfer between the casing and surroundings, for example by using external fans, or increasing the surface area, will be more effective at lowering the maximum temperature in the transducer stack with the new conductive layer than without. Without the new conductive layer the transfer of heat from the transducer stack to the casing is a clear bottleneck. With the new conductive layer this bottleneck is removed.

The new conductive layer could lead to some problems. The new layer is next to the electrode controlling the LF2 layer. It is therefore important that there either is an electrical insulator between the electrical insulator and the new layer. Another possible solution is to use a material that is thermally conductive but not electrical-lyconductive. An example of such a material is Aluminum Nitride with a thermal conductivity of 140-177 $\frac{W}{m \cdot K}$ [1].This layer also takes part of the place normally reserved for the transducer backing. If not properly designed it could therefore impact the ultrasound capabilities of the transducer stack. The new layer have to be able to work as a backing.

6. CONCLUSION

This thesis reviewed the power requirements for high Ultrasound Radiation Force apparatus, and the heat generation caused by this.

This thesis proposed a way to cool an ultrasound transducer. The cooling method is to have a an area on the casing of the transducer that has a high thermal conductivity, and a high emissivity. This layer is meant to passively transfer heat from the casing to the surroundings. This area on the casing is connected to the transducer stack through a copper layer that is separated for the stack by thermal paste. This cooling method was simulated using a two-step method. The first step was to determine the amount of heat transferred from the highly conductive area on the casing to the surrounding, assuming constant surface temperature. The second step was to simulate the heat transfer from the transducer stack to the casing assuming evenly distributed constant heat generation in the transducer stack.

The conductive casing that was simulated was a prism surrounding the sides of the transducer stack, but not the top and bottom. This prism was off height 4cm. It was found that the casing material should have as high conductivity and emissivity as possible in order to increase heat transfer. The thickness of thermal paste was found to have a large impact on the heat transfer from the transducer stack to the conductive casing. This necessitates care when applying thermal paste to make sure it has the desired thickness.

The warmest area of the transducer would, based on the simulations, be close to the backing. In order to increase heat transfer out of the transducer, it was therefore proposed to add a thermal conductive layer just above the backing off the transducer. This method was shown in simulations to be effective in increasing heat transfer. With this added thermal conductive layer the transducer would stabilize around $56C^o$ for a heat generation of 8.3W evenly distributed throughout the transducer.

6.1 Possibilities for further studies

Investigate the thickness of thermal paste required. The casing is not in direct contact with the transducer stack, but separated by a layer of thermal paste. This separation is to limit the casings effect on ultrasound generation, by increasing the rigidity of the transducer stack. It could be smart to check how thick the thermal paste would have to be in order for the transducer stack to be sufficiently isolated.

Investigate the possibility of using the new conductive layer as backing. The new conductive layer is in the position where the backing would usually be. It significantly increases heat transfer. However if it where to reduce the transducers applicability for ultrasound this method could not be used. It would therefore be useful to investigate if such a layer could fulfill the roles of a backing material as well as transfer heat.

Investigate the amount of heat generated. This thesis calculates the stable temperature that would be reached for a certain boundary temperature and heat generation. It does however not calculate how much heat would actually be generated in the transducer. It would be useful to calculate the heat generated to see if the methods proposed in this thesis are adequate for the transducer.

BIBLIOGRAPHY

[1] *Aluminum Nitride (AlN) - Properties and Applications, AZO materials, year = http://www.azom.com/article.aspx?ArticleID=610 - webpage visited in 05-08-2015.*

[2] *EN12464-1: The Lighting of Workplaces.* European Committee for Standardisation, 1990.

[3] *Introduction to COMSOL Multiphysics®.* Software manual created by Multiphysics, COMSOL, 1998-2015.

[4] *Materials and Coatings for Medical Devices: Cardiovascular.* Materials and processes for medical devices. ASM International, 2009.

[5] *Properties of Barium Titanate.* APC International LTD., https://www.americanpiezo.com/product-service/bati03.html - webpage visited in 10-08-2015.

[6] *Thermal Interface Materials For Electronics Cooling Products - Custom Solutions Catalog, T636 manufacturers specifications.* Parker Chomerics, http://vendor.parker.com/852568C80043FA7A/468ea5de5ac341d385257d390 05641c7/C118FE3366B55BA685256BD7004F6F0A/$FILE/THERMALMP.pdf - webpage visited in 05-08-2015.

[7] *Specification of Toshiba LED 5.4W lamp retrieved online.* http://web.archive.org/web/20110719165551/http://www.tlt.co.jp/tlt/new/lamp/hp_led/minikry_lda5.htm - webpage visited in 10-08-2015.

[8] *JunPus NANO DIAMOND THERMAL GREASE DX1 Manufacturers specifications, retrieved online.* http://www.junpus.com/thermal-paste/products/thermal-paste/item/76-nano-diamond-thermal-grease-dx1.html - webpage visited in 05-08-2015.

[9] *Introduction   to   Solar   Radiation.*   Newport   Corporation,   http://www.newport.com/Introduction-to-Solar-Radiation/411919/1033/content.aspx - webpage visited in 04-08-2015.

[10] B. Angelsen. *Ultrasound radiation force transport of drugs in tumors.* unpublished, Dept. of Circulation and Medical Imaging, NTNU, 2014.

[11] B. Angelsen and H.Torp. *Ultrasound Imaging Waves, Sigals and Signal processing in Medical Ultrasonics.* Emantec, 2000.

[12] K. J. Bathe. *Finite element procedures.* Klaus-Jurgen Bathe, 2006.

[13] K. J. Bathe and E. L. Wilson. Numerical methods in finite element analysis. 1976.

[14] S. W. Churchill and H. S. Chu. Correlating equations for laminar and turbulent free convection from a vertical plate. *International journal of heat and mass transfer*, 18(11):1323–1329, 1975.

[15] C. M. Counter. The roles of telomeres and telomerase in cell life span. *Mutation Research/Reviews in Genetic Toxicology*, 366(1):45–63, 1996.

[16] B. Alberts et al. *Molecular Biology of the Cell 4th Edition: International Student Edition.* Routledge, 2002.

[17] F. P. Incropera et al. *Fundamentals of Heat and Mass Transfer, sixth edition.* John Wiley & Sons, Inc, 2007.

[18] G. Dhatt et al. *Finite element method.* John Wiley & Sons, 2012.

[19] P. Koumoutsakos et al. The fluid mechanics of cancer and its therapy. *Annual review of fluid mechanics*, 45(1):325, 2013.

[20] S. Qin et al. Ultrasound contrast microbubbles in imaging and therapy: physical principles and engineering. *Physics in medicine and biology*, 54(6):R27, 2009.

[21] S. Sirsi et al. Effect of microbubble size on fundamental mode high frequency ultrasound imaging in mice. *Ultrasound in medicine & biology*, 36(6):935–948, 2010.

[22] D. Hanahan and R. A. Weinberg. Hallmarks of cancer: the next generation. *cell*, 144(5):646–674, 2011.

[23] Y. He. Heat capacity, thermal conductivity, and thermal expansion of barium titanate-based ceramics. *Thermochimica acta*, 419(1):135–141, 2004.

[24] M. Kaviany. *Principles of heat transfer*. John Wiley & Sons, 2002.

[25] T. Murphy. Maximum efficiency of white ligth. 2011.

[26] B. Pentenrieder. Finite element solutions of heat conduction problems in complicated 3d geometries using the multigrid method. *Master Thesis*, 2005.

[27] D. W. Siemann. The unique characteristics of tumor vasculature and preclinical evidence for its selective disruption by tumor-vascular disrupting agents. *Cancer treatment reviews*, 37(1):63–74, 2011.

[28] B. W. Stewart and C. P. Wild. *World Cancer Report 2014*. WHO, 2014.

[29] G. Wyszecki and W.S. Stiles. *Color Science: Concepts and Methods, Quantitative Data and Formulae*. Wiley Series in Pure and Applied Optics. Wiley, 2000.

[30] H. D. Young and R. A. Freedman. *University Physics* 12th *edition*. Pearson International Edition, 2008.